

Enrichment characteristics and sources of the critical metal yttrium in Zhijin rare earth-containing phosphorites, Guizhou Province, China

Xingxiang Gong^{1,2,3,4} · Shengwei Wu^{1,2} · Yong Xia^{1,2} · Zhengwei Zhang^{1,2} · Shan He^{1,2} · Zhuojun Xie^{1,2} · Jiafei Xiao^{1,2} · Haiying Yang^{1,5} · Qingping Tan^{1,2} · Yi Huang^{3,4} · Yuhong Yang^{3,4}

Received: 24 November 2020 / Revised: 28 December 2020 / Accepted: 3 February 2021 / Published online: 12 March 2021
© Science Press and Institute of Geochemistry, CAS and Springer-Verlag GmbH Germany, part of Springer Nature 2021

Abstract Yttrium (Y) is a critical metallic element that is used widely in modern scientific, technological, and industrial applications. Phosphorites in the Zhijin area of Guizhou Province, China, are famous for Y enrichment, but the enrichment characteristics and sources remain unclear. Previous studies suggested that the sources of rare earth elements (REEs, La–Lu) and Y (REYs, La–Lu+Y) were related to hydrothermal deposition. However, this study presents evidence refuting that hypothesis, with major and trace elemental data collected with quadrupole–inductively coupled plasma–mass spectrometry (Q–ICP–MS) analysis. These data show that Y in Zhijin REYs-containing phosphorites has a normal distribution and is

particularly enriched relative to other REYs. The Y enrichment degree is different at different \sum REY intervals. Specifically, the Y enrichment degree is higher at lower \sum REY values and lower at higher \sum REY values. The REYs-containing phosphorites show features of primary phosphorites. Both REEs and Y have good correlations with P_2O_5 in the phosphorites with low REYs contents (total REYs < 535 ppm), whereas at high REYs contents (total REYs \geq 535 ppm), REEs have a good correlation with P_2O_5 but Y does not. Inconsistent enrichment processes of REYs are suggestive of complex sources of Y. Thus, seafloor hydrothermal fluids were not the direct source of Y. Normal seawater mixed with terrestrial sources might have contributed to the origin of Y here. This study could lead to improvements in Y mineral resource explorations and the situation involving the global REYs supply crisis.

Xingxiang Gong and Shengwei Wu contribute equally to this work.

Electronic supplementary material The online version of this article (<https://doi.org/10.1007/s11631-021-00460-8>) contains supplementary material, which is available to authorized users.

✉ Yong Xia
xiayong@mail.gyig.ac.cn

Xingxiang Gong
gongxingxiang@mail.gyig.ac.cn

- ¹ Institute of Geochemistry, Chinese Academy of Sciences, Guiyang 550081, China
- ² University of Chinese Academy of Sciences, Beijing 100049, China
- ³ Technology Innovation Center of Mineral Resources Explorations in Bedrock Zones, Ministry of Natural Resources, Guiyang 550081, China
- ⁴ Reserve Bureau of Land and Mineral Resources of Guizhou Province, Guiyang 550081, China
- ⁵ School of Earth Sciences, Yunnan University, Kunming 650500, China

Keywords Yttrium · Phosphorites · Rare earth elements · Trace elements · Enrichment processes

1 Introduction

The atomic number of yttrium (abbreviated as Y) is 39, the relative atomic weight is 89, the outer electron arrangement is $4d^1 5s^2$, and its common valence is 3. Because the chemical properties of Y are similar to those of rare earth elements (REEs), Y is classified as an REE. Y has been used widely in glass, alloys, televisions, and the iron and steel industries in recent decades, and nowadays, this metal has become a critical element in modern scientific, technological, and industrial applications.

Y often display itinerant properties of nature. In terms of a difference in stability or extraction properties, Y can

occupy almost any position in the lanthanides. With different ligands, Y will display different properties. Y resembles a light REE for soft ligands; however, Y resembles a heavy REE for hard ligands (Borkowski and Siekierski 1992).

Many marine phosphorites are known for their enrichment of REYs (REEs and Y) during the early diagenesis phase (Hein et al. 2016). The main mineral of phosphorites is francolite, and its composition can be summarized as $(\text{Ca}, \text{Na}, \text{Mg}, \text{Sr})_{10}(\text{PO}_4, \text{CO}_3, \text{SO}_4)_6\text{F}_2$ (McArthur et al. 1980; McArthur 1986). The REYs such as REE^{3+} and Y^{3+} , as well as SiO_4^{4-} can replace Ca^{2+} and PO_4^{3-} ($\text{REE}^{3+} + \text{SiO}_4^{4-} = \text{Ca}^{2+} + \text{PO}_4^{3-}$) and then enter the lattice of apatite by isomorphic substitution (Jiang et al. 2020).

The REYs (especially Y) enrichment of Zhijin phosphorites in China has attracted the attention of numerous people. Many scholars (e.g., Chen 2013, 2019; Duan et al. 2015; Guo et al. 2017; Wu 2019; Xia et al. 2019; Xu 2019; Zhang et al. 2007a, 2007b) have carried out studies on the relationship between REEs and P, and Y and P. These studies focused principally on the state of occurrence, geochemical characteristics, enrichment characteristics, and paleogeographic environment of REYs-bearing phosphorites.

Previous main views are as follows:

- (1) In terms of occurrence state, REYs enriched principally in the sandy clastic phosphorites and the dark-colored parts of the layered structural phosphorites in the lower part of the Gezhongwu Formation ($\text{C}_{1\text{gz}}$) (Guo et al. 2017), which stratigraphic age considered to be between $(522.9 \pm 8.6) - (535.2 \pm 1.7)$ Ma (Xia et al. 2019). These REYs do not exist in the form of independent minerals, but are associated closely with apatite (Guo et al. 2017), and existed principally in collophane in the form of isomorphism (Zhang et al. 2007a, b).
- (2) As far as the distribution patterns of Rare Earth are concerned, REYs showed negative Ce anomalies, positive Gd anomalies, Y enrichment, and other heavy rare earth elements (HREEs) depletion (Wu et al. 2019; Wu 2019).
- (3) REYs enrichment is related to the geographical microfacies. Xia et al. (2019) and Xu (2019) divided the paleogeographic environment of the Early Cambrian phosphorite-forming period in the Zhijin area into gentle slope basin, gentle slope beach, and gentle slope edge areas (the areas were also divided into front and back edges) according to the features of the rock structure and mineral size, grinding roundness, sorting characteristics, and so forth. The results showed that the different geographical microfacies have different degrees of REYs enrichment.
- (4) Some signatures of hydrothermal deposition were showed (Guo 2017).

Previous studies have led to a certain understanding of the occurrence state and enrichment characteristics of REYs in phosphorites, and establish an important basis for this study. However, the enrichment characteristics and sources of Y remain unclear. To reveal the enrichment characteristics and sources of Y in the Zhijin area, the major and trace element concentrations of Y-rich phosphorite samples in this area were measured, and a cluster analysis and factor analysis of the REYs data was then carried out. This study allows us to gain insight into the enrichment characteristics and sources of Y, offer useful guidance for Y mineral resource explorations, and provide the possibility to ease the crisis of the global REYs (especially Y) supply crisis.

2 Geological background

The Yangtze platform is probably the largest phosphate basin in the world (Ilyin 1998). The Zhijin REYs-bearing phosphorite deposit is located at the southwestern end of the central Guizhou uplift in the passive fold belt in the southern part of the Upper Yangtze Old Continent. From old to new, the outcrop strata are as follows: Upper Sinian Dengying Formation, Lower Cambrian Gezhongwu Formation ($\text{C}_{1\text{gz}}$), Niutitang Formation and Mingxinsi Formation, Lower Carboniferous Jiujiang Formation and Dapu Formation, Middle Permian Liangshan Formation, Qixia Formation, and Maokou Formation, Upper Permian Emeishan Basalt, Longtan Formation, Changxing Formation, and Dalong Formation, Lower Triassic Yelang Formation, Jialingjiang Formation, Middle Triassic Guanling formation, and Quaternary. Missing strata include the Paleozoic Upper Cambrian, Ordovician, Silurian, Devonian, and Mesozoic Jurassic and Cretaceous; magmatic rocks are not developed (Li et al. 2008; Xia et al. 2019; Yang et al. 2013). The tectonic lines in the area are extended toward the northeast direction, and the structural deformations are dominantly faults, followed by folds (Li et al. 2008). Previous studies (Xia et al. 2019) have revealed that the relationship between the phosphorite deposition and structures in this area is not obvious, but the relationship between the phosphorite deposition and sedimentary paleogeographic settings is obvious. The Lower Cambrian Gezhongwu Formation ($\text{C}_{1\text{gz}}$) is the regional phosphorite-bearing stratum. Host-Y minerals, namely, apatite, can be found in the Lower Cambrian Gezhongwu Formation ($\text{C}_{1\text{gz}}$).

The investigated area is located in the western margin of the Yangtze platform (Fig. 1, modified according to Chen

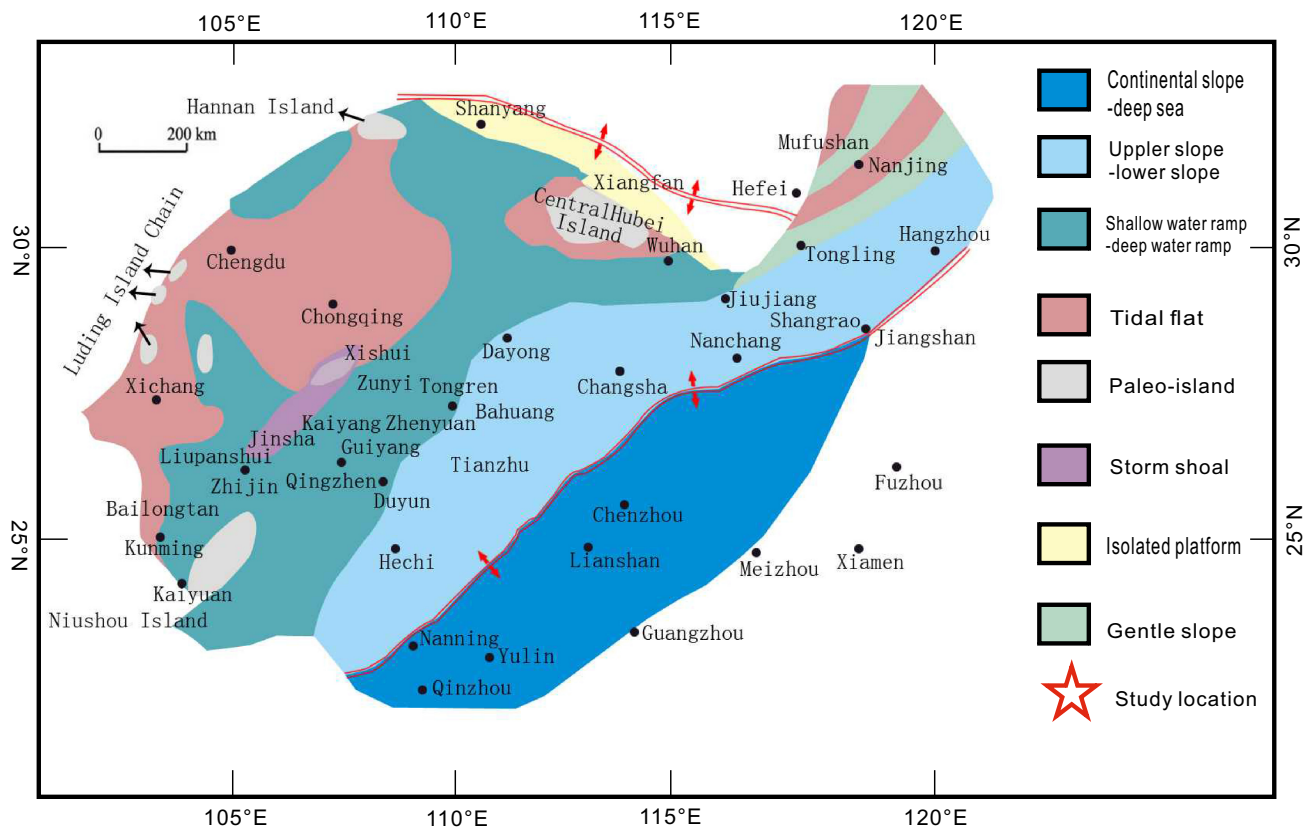


Fig. 1 Early Cambrian Paleogeography Map in Yangtze Platform (Modified After Chen et al. 2013)

et al. 2013). During the Early Cambrian period, the paleogeography was generally a gentle slope composed of carbonates and phosphates. Xia et al. (2019) studied the horizontal changing characteristics of sedimentary basins and found that, from west to east, the sedimentary basins can be roughly divided into the back edge of a gentle slope basin, the front edge of a gentle slope basin, gentle slope beach, the front edge of a gentle slope beach (Fig. 2). These microfacies affected the enrichment of phosphorites and REYs, so that the upper and lower section of the profile shows different characteristics. The characteristics of the vertical change are as follows: the lower part is principally columnar, with strip and conical colloidal phosphate particles, and there are a small number of circular particles and biological particles; the sorting property and grinding roundness of the particles are medium to poor. Additionally, the upper part is principally granular particles, and the sorting property and grinding roundness of the particles are better in this location. As a result, the vertical hydrodynamic strength reflected by the structural characteristics of the section differs such that the lower part's strength is lower than that of the upper part, and laterally the hydrodynamic strength of the middle part of the basin is lower than that of the basin edge (Xia et al. 2019; Xu 2019).

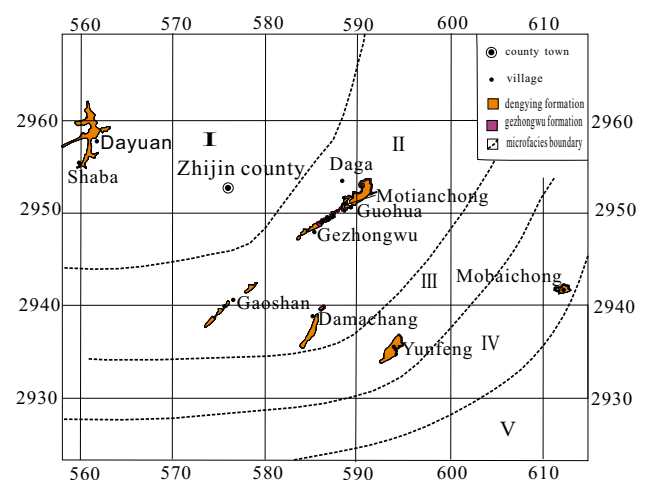


Fig. 2 Paleogeographic microfacies map of Zhijin REY-bearing phosphorite area (Modified according to Xu 2019). **I** Backward edge of gentle slope basin. **II** Gentle slope basin. **III** The front edge of gentle slope basin and the back edge of gentle slope beach. **IV** gentle slope beach. **V** The front edge of the slow slope beach

3 Characteristics of the mineral deposit

3.1 Characteristics of the strata-bearing ore

The series of REYs-containing phosphorites is principally located in the Gezhongwu Formation (ϵ_{1gz}) (Fig. 3), which is underlay by the phosphorus-containing (REYs) Niutitang Formation (ϵ_{1n}) and overlay by carbonate dolostone of the Dengying Formation (Z_2dy^2).

The Dengying Formation (Z_2dy^2) is the direct base of the Gezhongwu Formation (ϵ_{1gz}) in the ore-bearing rock

series. It is a medium-thick fine-grained dolomite layer with colors of gray, light gray, and grayish-white.

The Niutitang Formation (ϵ_{1n}) is a fine-grained feldspar-quartz sandstone, silty sandy carbonaceous mudstone, and tuberculate, lenticular siliceous phosphorite-REYs ore layer. In the Niutitang Formation (ϵ_{1n}), the concentrations of phosphorite and REYs change obviously.

The ore-bearing rock series is namely the Gezhongwu Formation (ϵ_{1gz}), which is the main phosphorus-containing (REYs) ore layer with a thickness of 0–33.73 m. The main features of the Gezhongwu Formation (ϵ_{1gz}) are as follows.

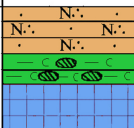
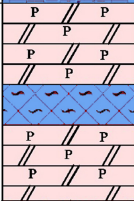

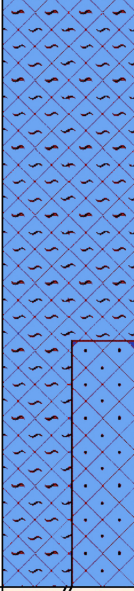
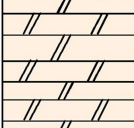
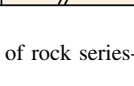
Formation code	Histogram	Brief description of rock and ore characteristics
ϵ_{1n}		Gray black thin-layer carbonaceous mudstone or carbonaceous shale.
ϵ_{1gz}		Layered, tuberculous, lenticular siliceous phosphate rock - rare earth ore.
		i.e. B ore layer. It is mainly gray, dark gray medium-thick layer fine-grained bearing-phosphorous dolomite. The thickness ranges from 0 to 7.70m. And it developed only locally. The P_2O_5 content is 2.37–18.67 percent, generally 5–11 percent.
		That is A ore layer and mainly striped phosphorite. The thickness is 2.08–31.57 m. It is unequal thick interbed composed of pale gray thin layered containing-rare earth dolomite phosphorite (thickness is 2–15cm and usually is 2–5cm) and dark gray medium to thick layered fine-grained phosphorous dolomite (20–50cm thick). The P_2O_5 content is 5.23–24.94 percent with an average of 17.62 percent, Average REE $_2O_3$ content is 0.1034 percent, Y $_2O_3$ is 0.0370 percent.
Z_2dy^2		Sandy clastic phosphorite-rare earth sub-deposit layers. The ore is massive. The content of P_2O_5 is 12.12–37.39 percent, the content of REE $_2O_3$ is 0.142 percent.
		Gray, light gray, grayish white meddle to thick layered fine-crystalline dolomite.

Fig. 3 Synthesis histogram of rock series-containing phosphorus(rare earth) (Modified After Meng et al. 2016; Wu 2019))

- (1) Phosphorus-bearing dolomite (ore layer B). This layer is composed of gray-dark gray, medium to thick layered fine-grained bearing-phosphorus dolomite. Its thickness ranges from 0 to 7.70 m (locally the section is not well developed). The P_2O_5 has a concentration of 2.37%–18.67% (generally 5%–11%). The middle part of this layer developed only in the Guohua section and Dajia section of Xinhua phosphorite, where a continuous strip-shaped dolomitic phosphorite-REYs ore layer (namely ore layer B) is developed. For ore layer B, the monolayer thickness is 0.93–9.12 m, the average thickness is 3.14 m; the average P_2O_5 grade is 18.67%, and the content of REEs (REE_2O_3) is 0.1%.
- (2) Phosphorites with an unequal thick banded structure (ore layer A). It is a Dark gray medium to thick layered fine-grained containing-phosphorus dolomite layer, with a thickness that ranges from 20 to 50 cm, interbedded with a dark gray thin layer of dolomitic containing-REYs phosphorite layer of a thickness of 2–15 cm. Thus, it forms a banded structure with unequal thickness. This layer is the main phosphorite (REYs) ore layer in the exploration area (ore layer A). In the mineral warrant area, the thickness of this layer is 2.08–31.57 m, with a typical value of 8 m. The original ore in this layer has a low P_2O_5 concentration of 5.23%–24.94%, with an average P_2O_5 concentration of 17.62%, an average REE_2O_3 content of 0.1034%, and an average Y_2O_3 content of 0.0370%. Because of surface weathering, the P_2O_5 is relatively enriched and forms a strip-like dolomitic bearing-REYs phosphorite ore layer with high P_2O_5 concentrations. The bottom of this layer is located in the exploration warrant area of the Motianchong Phosphorite Mine in the Guohua section of Xinhua phosphorite. At the bottom of this layer, the original ore is massive, the thickness is 0–14.67 m, the P_2O_5 concentration is 12.12%–37.39%, and the REE_2O_3 content is 0.142%. However, the bottom of this layer is poorly developed in the other areas (Meng et al. 2016).

3.2 Ore characteristics

The REYs occur principally in phosphorites. There are nine ore sections (Meng et al. 2016; Wu 2019), such as Xinhua, DaMaChang, GaoShan, DaJia, Guohua.

The REYs-containing phosphorite minerals are principally light gray, gray, gray-black, black, brown-yellow. Phosphorites usually show sandy-clastic (Fig. 4C1), which are locally carbonaceous (Fig. 4C1). Calcite, dolomite

(Fig. 4A2), and siliceous cementation (Fig. 4B2) occur commonly.

3.3 Mineralogical characteristics

The main mineral of REYs-bearing phosphorite is apatite, the gangue mineral mainly consists of dolomite, quartz, and clay minerals. There is usually a growth-decline relationship between concentrations of ore minerals and concentrations of gangue minerals, that is, when the concentrations of apatite are high, the concentrations of dolomite, quartz, and clay minerals are usually low. In contrast, when the concentrations of apatite are low, the concentrations of dolomite, quartz, and clay minerals are usually high (Fig. 4).

In addition to the main ore minerals and gangue minerals, secondary minerals such as pyrite and hematite are often found in phosphorites. Zircon, rutile, barite, spinel, sphalerite, galena, siderite, pyrolusite, and other Cr- and Na-bearing minerals also appear locally in the phosphorites.

4 Sampling and testing methods

In the study, we selected representative Y-rich phosphorite samples from the Zhijin Gezhongwu Formation (C_{1gz}) in Guizhou Province. All of the samples were collected from drillcore samples obtained in a borehole section, and the profile direction is mainly toward NW–SE orientation. The borehole numbers of samples were as follows: ZK1802, ZK2802, ZKX202, ZK2601, ZK2603, ZK2204, ZK2604, and ZKX001. A total of 150 phosphorite samples were collected. In general, the sampling distance was 1 m.

After sampling, the major elements were analyzed by melting the samples (melting temperature is at 1000 °C) with lithium borate or lithium borate-lithium nitrate and then carrying out XRF analyses. The detection limit was 0.01%, and the relative standard deviation was better than 5%.

After decontamination and drying, the whole rock samples were ground into 200 mesh powder. Then, the trace element analyses were carried out. After high temperature (1000 °C) and high-pressure reduction by the acid-solution method, the contents of trace elements were quantified by Q-ICP-MS analyses in the State Key Laboratory of Ore Deposit Geochemistry at the Institute of Geochemistry, Chinese Academy of Sciences (IGCAS). The model number of the apparatus was ELANDRC-e. The relative standard deviation was better than 10% (Chew et al. 2016) (Figs. 5, 6).

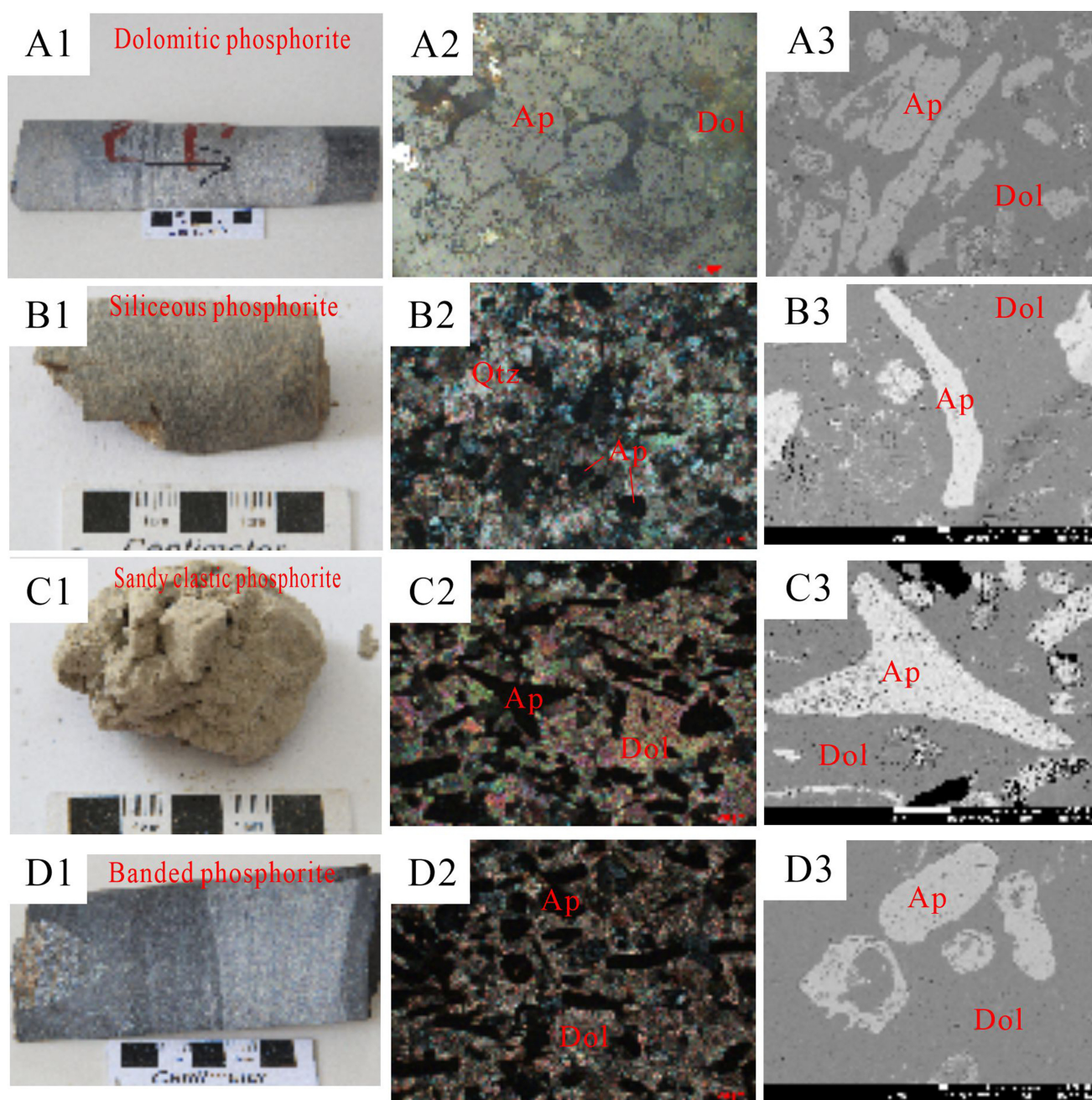


Fig. 4 Characteristics of Early Cambrian phosphorite in Zhajin region. **A** dolomitic phosphorite. **B** siliceous phosphorite. **C** sand clastic phosphorite. **D** banded phosphorite. Number 1 for hand specimen. Number 2 for microscope. Number 3 for scanning electron microscope(SEM). *Ap* denotes apatite. *Dol* denotes dolomite. *Qtz* denotes quartz

Through these tests, 15 REYs and 28 other major and trace elements were analyzed, including V, Cr, Co, Ni, Cu, Zn, Ga, Ge, As, Rb, Sr, Zr, Nb, Mo, Ag, Cd, Sb, Ba, W, Pb, Th, U, Al_2O_3 , CaO , F, MgO , MnO_2 and P_2O_5 was determined.

Based on the tests for major and trace elements, analysis charts were drawn by using Mapgis and Photoshop. We used SPSS and Origin software to analyze the test data. The relevant parameters of the factor analysis were set as

follows: (1) extraction method: principal component analysis; (2) analysis: correlation coefficient matrix; (3) rotation: maximum variance; (4) convergence maximum: 25 iterations; (5) factor analysis: regression analysis; (6) principal component analysis using the default method.

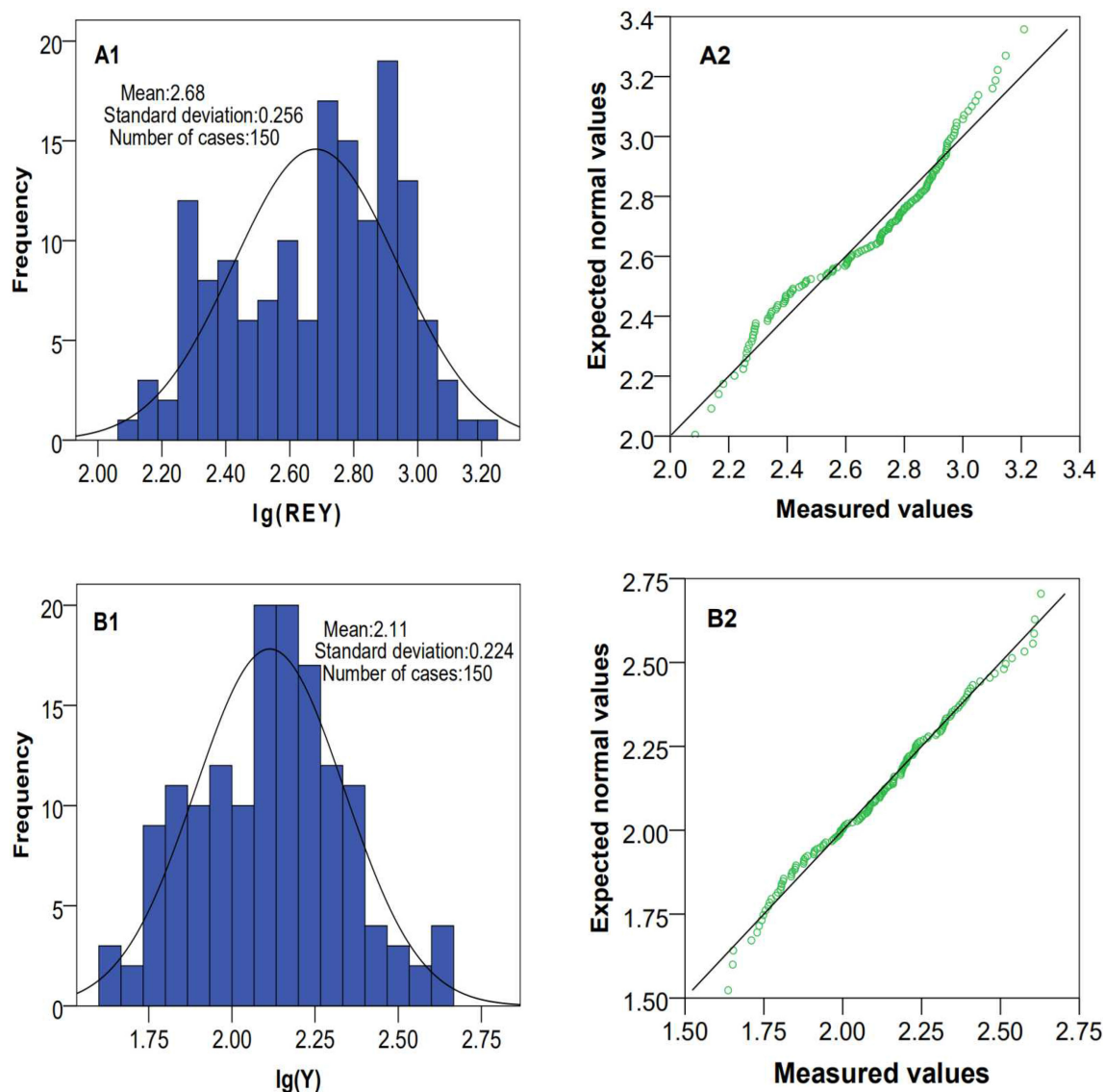


Fig. 5 The characteristic plots of $\lg(\Sigma REY)$ and $\lg(Y)$. **A1** frequency plot of $\lg(\Sigma REY)$. **A2** normal Q-Q plot of $\lg(\Sigma REY)$. **B1** frequency plot of $\lg(Y)$. **B2** normal Q-Q plot of $\lg(Y)$

5 Enrichment characteristics of Y

5.1 Statistical characteristics

The samples collected in this study are phosphorites, which came from the same ore district and the same stratum in the Zhijin region. Previous studies (Yang et al. 1995) have indicated that Y principally occurs here in apatite. Xu et al. (2019) found that the Y content is positively correlated with the P_2O_5 concentration in phosphorites, and it was proposed that the Y content may be closely related to the chemical and mineral composition of the phosphorites in the phosphorites and the enrichment of Y may have resulted from the preferential absorption of Y relative to other lanthanides. As research has progressed, it is believed

that the concentration of the major elements in geological samples obeys a normal distribution, and the logarithmic values of contents of trace elements obey a normal distribution on the whole (Stine 2016; Tan and Wang 2017; Tan et al. 2018). To study the characteristics of the major elements, trace elements, and REYs in Zhijin phosphorites, the contents of trace elements and the total amount of REYs were log-transformed, while the concentrations of major elements were not log-transformed.

Statistical distribution features of the data can be expressed as frequency distribution histograms and normal Q-Q (quantile–quantile) graphs. The frequency distribution histograms and normal Q-Q plots of the sample data were drawn by using SPSS software. The confidence intervals were set as 95%. The quartile and median of the samples

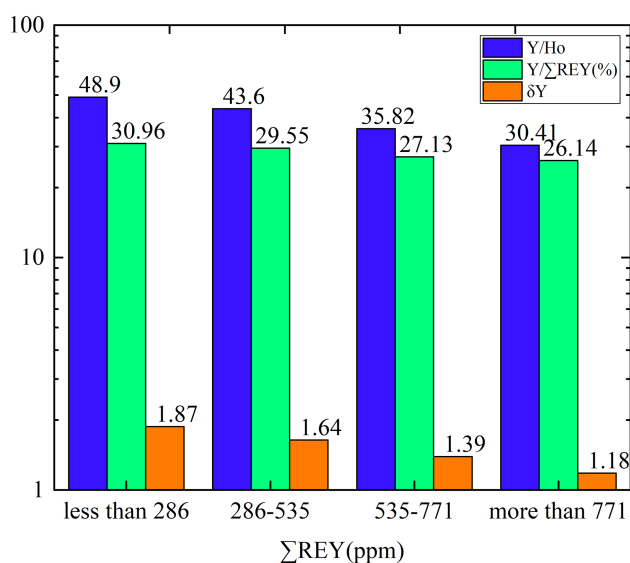


Fig. 6 $Y/\Sigma REY$ (%), δY and Y/Ho (medians) variation plots of different ΣREY intervals

were calculated according to ΣREY scope, and these values amounted to 286 ppm (25%), 535 ppm (50%), and 771 ppm (75%), respectively. According to the ΣREY scope, the samples were divided into four sections, that is, ΣREY values less than 286 ppm, values ranging from 286 to 535 ppm, values ranging from 535 to 771 ppm, and values more than 771 ppm.

The statistical results of the sample data are listed in Table 1, and the distribution pattern is shown in Fig. 7. Here, the ΣREY represents the total contents of the REEs and Y. δEu is the abnormality of europium calculated by the formula $\delta Eu = Eu/Eu^* = Eu_N/(Sm_N \times Gd_N)^{0.5}$ (Taylor and McLennan 1985), and δY is the abnormality of yttrium

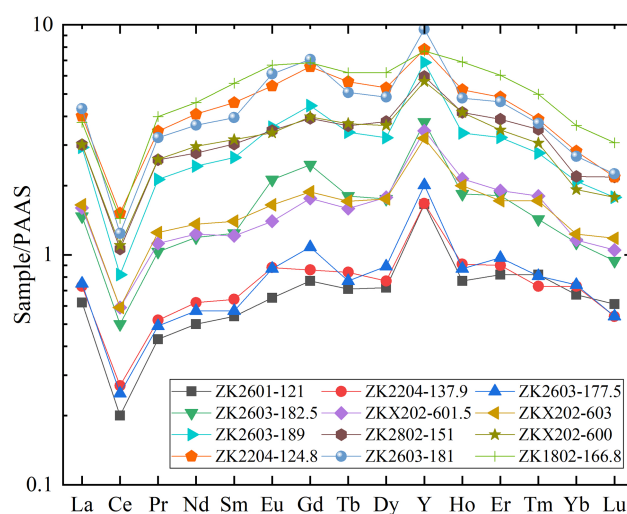


Fig. 7 REY distribution pattern of Zhijin phosphorite-rare earth

calculated by formula $\delta Y = 2Y_N/(Dy_N + Ho_N)$ (Fazio et al. 2007) (Y inserted between Dy and Ho based on radius sizes). Er/Nd , Y/Ho , and $(La/Sm)_N$ are ratios of certain REEs, where the subscript N denotes Normalized to Post-Archean Australian shale (PAAS) (McLennan 1989) values.

The statistical characteristics of the samples are shown in Fig. 5. Figure 5A1, B1 presents the frequency distribution histograms of the contents of REYs and Y in the phosphorite, respectively. Figure 5A2, B2 presents the normal Q-Q graphs of the contents of REYs and Y in the phosphorite, respectively. The data for REYs and Y of the samples within the Q-Q diagram was located near the straight line of Q-Q graphs. The data for REYs and Y of the samples showed normal distribution characteristics.

Table 1 Some elemental Characteristics of Early Cambrian phosphorite in Zhijin Region

REY scope(ppm)		$Y/\Sigma REY(\%)$	δEu	δY	Er/Nd	$(La/Sm)_N$	Y/Ho	Er_N/Lu_N	MgO(%)	CaO/ P_2O_5	(CaO + MgO)/ P_2O_5
Less 286	Median	30.96	1.04	1.87	1.45	1.20	48.90	1.25	15.90	8.01	12.40
	Max	37.10	1.26	2.34	1.69	1.43	66.22	1.50	18.15	17.76	29.13
	Min	25.67	0.90	1.37	1.04	0.91	35.67	0.99	6.00	4.52	5.93
286–535	Median	29.55	1.00	1.64	1.30	1.10	43.60	1.93	13.68	3.73	5.23
	Max	35.77	1.27	2.38	1.63	1.33	66.71	2.48	17.60	6.17	9.56
	Min	16.74	0.88	0.76	1.11	0.73	20.81	1.46	7.49	2.30	2.94
535–771	Median	27.13	1.02	1.39	0.11	1.05	35.82	2.05	10.53	2.44	3.19
	Max	38.49	1.24	2.59	0.13	1.40	72.18	2.42	14.70	3.22	4.47
	Min	14.86	0.12	0.69	0.10	0.68	18.53	1.74	3.26	1.54	1.67
Greater 771	Median	26.14	1.01	1.18	0.10	0.87	30.41	2.23	4.90	1.66	1.86
	Max	35.97	1.33	2.47	0.13	1.19	67.53	2.59	11.05	2.58	3.37
	Min	14.39	0.87	0.57	0.09	0.54	15.82	1.86	0.33	1.36	1.38

5.2 Enrichment characteristics of yttrium

In this study, the enrichment degree of Y can be expressed by the percentage of Y in $\sum\text{REY}$ (Y/REY), the Y anomaly (δY), the Y/Ho ratio, and the REYs distribution pattern. The percentage of Y was found to be very high relative to other REYs, but this percentage was not constant. With $\sum\text{REY}$ values increasing from low to high, the percentage of Y in $\sum\text{REY}$ gradually decreased. When the $\sum\text{REY}$ value rose from less than 286 to 286–535 ppm, 535–771 ppm, and greater than 771 ppm, the percentage of Y (median) decreased from 30.96% to 29.55%, 27.13%, and 26.14%, respectively. As the $\sum\text{REY}$ value changed from the smallest value (less than 286 ppm) to the largest value (greater than 771 ppm), the percentage of Y in $\sum\text{REY}$ (median) decreased by 16% (Fig. 6). This finding suggests that the Y enrichment degree decreases with increasing $\sum\text{REY}$ values.

On the whole, the Zhijin phosphorite shows a positive Y anomaly, but this anomaly was found to vary. When $\sum\text{REY}$ increased from low to high, the Y anomaly δY decreased. When $\sum\text{REY}$ rose from less than 286 ppm to 286–535 ppm, 535–771 ppm, and greater than 771 ppm, the Y anomaly δY (median) decreased from 1.87 to 1.64, 1.39, and 1.18, respectively. From the smallest $\sum\text{REY}$ interval to the largest $\sum\text{REY}$ interval, the Y anomaly δY (median) decreased by 37% (Fig. 6). This indicates that with an increase in $\sum\text{REY}$, the abnormal changes of Y relative to Dy and Ho decrease, and the behavior of Y tends to be consistent with that of Dy and Ho.

The trend in which the Y anomaly decreased with the $\sum\text{REY}$ value was also reflected in the Y/Ho data. When the $\sum\text{REY}$ rose from less than 286 ppm to 286–535 ppm, 535–771 ppm, and greater than 771 ppm, the Y/Ho ratio (median) decreased from 48.90 to 43.60, 35.82, and 30.41, respectively. When $\sum\text{REY}$ increased from the smallest value (less than 286 ppm) to the largest value (greater than 771 ppm), the Y/Ho ratio (median) decreased by 38% (Fig. 6). This finding indicates that, with the increase in $\sum\text{REY}$, the abnormal change of Y relative to Ho becomes smaller, and the behavior of Y becomes gradually consistent with that of Ho.

The degree of variation of Y anomalies also can be illustrated in the REYs distribution patterns. Table 2 shows some PAAS-normalized values of REYs selected from random samples. According to Table 2, the REYs distribution pattern plots of Zhijin phosphorite were obtained (Fig. 7). As shown in the plots, Zhijin REYs-bearing phosphorites are generally characterized by a cap-shaped REYs distribution pattern, negative Ce anomalies, no Eu anomalies, middle rare earth elements (MREEs) enrichment, and Y special enrichment. The diagram also revealed that, relative to Dy and Ho, when the $\sum\text{REY}$ value was

smaller (as shown in samples ZK2601-121, ZK2204-137.9, and ZK2603-177.5), the Y anomaly was larger, and when the $\sum\text{REY}$ value was larger (as shown in samples ZK2603-181 and ZK1802-166.8), the Y anomaly was smaller. This finding indicates that the degree of Y enrichment decreases with the increase in $\sum\text{REY}$.

As a consequence, whether from the perspective of percentages of Y in $\sum\text{REY}$ (Y/REY) and the Y anomalies (δY) or the Y/Ho ratios and the REYs distribution patterns, Zhijin REYs-bearing phosphorites show Y-enrichment characteristics, but the enrichment degree of Y decreases as the $\sum\text{REY}$ value increases from low to high.

6 Cluster analyses and factor analyses

6.1 Cluster analyses

Figure 8 presents a chart of the cluster analysis of different REYs contents of Zhijin phosphorites. In the chart, the horizontal coordinate is the square Euclidean distance, and the vertical coordinate is the combination characteristic of different elements. By using the square Euclidean distance 5 as the upper limit, the square Euclidean distance between 0 and 5 is indicative of the close relationship between the elements, i.e., the farther from the square Euclidean distance 5, the more estrangement there is between the elements.

As shown in Fig. 8, for the phosphorite, when the total REYs content was less than 286, the square Euclidean distance between P_2O_5 , F, REE, and Y was between 0 and 5, which suggests that the enrichment of REE and Y were closely related to the P_2O_5 . This is consistent with the conclusion of some of the previous discussions in this article that suggested that the enrichment of REYs is closely related to the apatite concentration. Namely, a higher apatite concentration is associated with a higher REYs content.

When the REYs content in phosphorites was between 286 and 535 ppm, the square Euclidean distance between P_2O_5 , F, CaO, REE, and Y was 0–15, where the P_2O_5 , F, CaO components represent the apatite composition, thereby denoting that the REE and Y enrichment was closely related to the apatite concentration. However, compared with the phosphorites with the content of REYs less than 286 ppm, the square Euclidean distance between element Y and P_2O_5 , F, Sr, REE was 5–15, which indicated that the correlations between Y and P_2O_5 , F, Sr, REE had decreased.

When the content of REYs in phosphorites was 535–771 ppm, the square Euclidean distance between P_2O_5 , F, REE, CaO was between 0 and 10, and the results suggested that while there were close relations between

Table 2 PAAS-normalized values of rare earth elements in some samples

Samples	La	Ce	Pr	Nd	Sm	Eu	Gd	Tb	Dy	Y	Ho	Er	Tm	Yb	Lu
ZK2601-121	0.62	0.20	0.43	0.50	0.54	0.65	0.77	0.71	0.72	1.66	0.77	0.82	0.82	0.67	0.61
ZK2204-137.9	0.73	0.27	0.52	0.62	0.64	0.88	0.86	0.84	0.77	1.67	0.91	0.90	0.73	0.73	0.54
ZK2603-177.5	0.75	0.25	0.49	0.57	0.57	0.87	1.08	0.77	0.89	2.01	0.87	0.97	0.81	0.74	0.54
ZK2603-182.5	1.47	0.50	1.03	1.19	1.24	2.12	2.46	1.80	1.75	3.78	1.84	1.81	1.43	1.13	0.94
ZKX202-601.5	1.60	0.59	1.12	1.23	1.21	1.40	1.76	1.59	1.78	3.46	2.14	1.90	1.80	1.16	1.05
ZKX202-603	1.65	0.59	1.25	1.36	1.40	1.65	1.88	1.71	1.75	3.21	2.00	1.72	1.72	1.23	1.18
ZK2603-189	2.93	0.82	2.13	2.43	2.65	3.59	4.45	3.41	3.23	6.86	3.38	3.24	2.77	2.09	1.78
ZK2802-151	3.01	1.06	2.59	2.77	3.03	3.47	3.92	3.64	3.80	5.96	4.16	3.89	3.51	2.19	2.18
ZKX202-600	3.01	1.10	2.60	2.96	3.17	3.39	3.98	3.72	3.65	5.67	4.16	3.49	3.06	1.92	1.78
ZK2204-124.8	4.01	1.52	3.45	4.09	4.59	5.42	6.57	5.66	5.32	7.82	5.22	4.85	3.88	2.82	2.18
ZK2603-181	4.32	1.24	3.23	3.66	3.95	6.12	7.07	5.08	4.85	9.57	4.80	4.63	3.73	2.68	2.25
ZK1802-166.8	3.77	1.44	3.99	4.59	5.57	6.68	6.84	6.19	6.20	7.70	6.90	6.04	4.99	3.65	3.07

elements, there was no correlation between Y and P_2O_5 . When the content of REYs in phosphorites was more than 771 ppm, the results also indicated that there was no correlation between element Y and P_2O_5 .

Therefore, the Y enrichment is inconsistent with the REE enrichment. For the Zhijin phosphorites with a lower REYs content (total REYs < 535 ppm), both REEs and Y showed good correlations with P_2O_5 , whereas for those with a higher REYs content (total REYs \geq 535 ppm), REEs also had a good correlation with P_2O_5 , but Y showed no correlation with P_2O_5 .

6.2 Factor analyses

The results of the cluster analysis indicated that for Zhijin phosphorites with a lower REYs content (< 535 ppm), both REEs and Y had good correlations with P_2O_5 . For those with a higher REYs content (\geq 535 ppm), REEs also had a good correlation with P_2O_5 , but Y showed no correlation with P_2O_5 . Therefore, based on the cluster analysis, two-factor analyses were respectively carried out for the phosphorites with a lower REYs content (< 535 ppm) and higher REYs content (\geq 535 ppm), which allowed for the study of the differences in REYs enrichment of the phosphorites with different REYs contents.

Results for the Kaiser–Meyer–Olkin (KMO) tests and Bartlett spherical tests of the factor analysis data for Zhijin phosphorites with a lower REYs content (< 535 ppm) and higher REYs content (\geq 535 ppm) are shown in Table 3. As a rule, for factor analysis, the best effect occurs when KMO statistics values are greater than 0.9, and results are acceptable when KMO statistics values are between 0.7 and 0.9, but results are not suitable when KMO statistics values are less than 0.5 (George and Mallery 2019). In this

study, for the factor analyses of the phosphorite samples with a lower REYs content (< 535 ppm) and higher REYs content (\geq 535 ppm), the KMO values were 0.752 and 0.841, respectively, which is considered suitable for factor analysis. For phosphorites with both a lower REYs content (< 535 ppm) and higher REYs content (\geq 535 ppm), the significance values of Bartlett spherical tests of the factor analyses were less than 0.01. This indicates that there are significant correlations between variables.

Tables 4 and 5 present the explanation lists of total variance for the factor analyses of the Zhijin phosphorite samples with a lower REYs content (< 535 ppm) and higher REYs content (\geq 535 ppm), respectively. The explanation lists of total variance consist of three parts, namely, the various interpretations of the eigenvalues of initial factors, the extracted load factors, and the rotating load factors.

The variance interpretations of the eigenvalues of initial factors provide the variances explained by each factor and their sum of accumulation. In observations of the eigenvalues of initial factors of the phosphorites with a lower REYs content (< 535 ppm), the eigenvalues of the first seven factors were found to be all greater than 1, and the cumulative variance interpreted reached more than 80%; hence, extraction of these seven factors can best explain the information contained in the original variables. By the same token, for the phosphorites with a higher REYs content (\geq 535 ppm), the eigenvalues of the first six factors were found to be all greater than 1, and the cumulative variance interpreted reached more than 83%; hence, the extraction of these six factors can best explain the information contained in the original variables. The variance interpretation of the extracted load factors is namely the interpretation for the total variance by the extracted factors

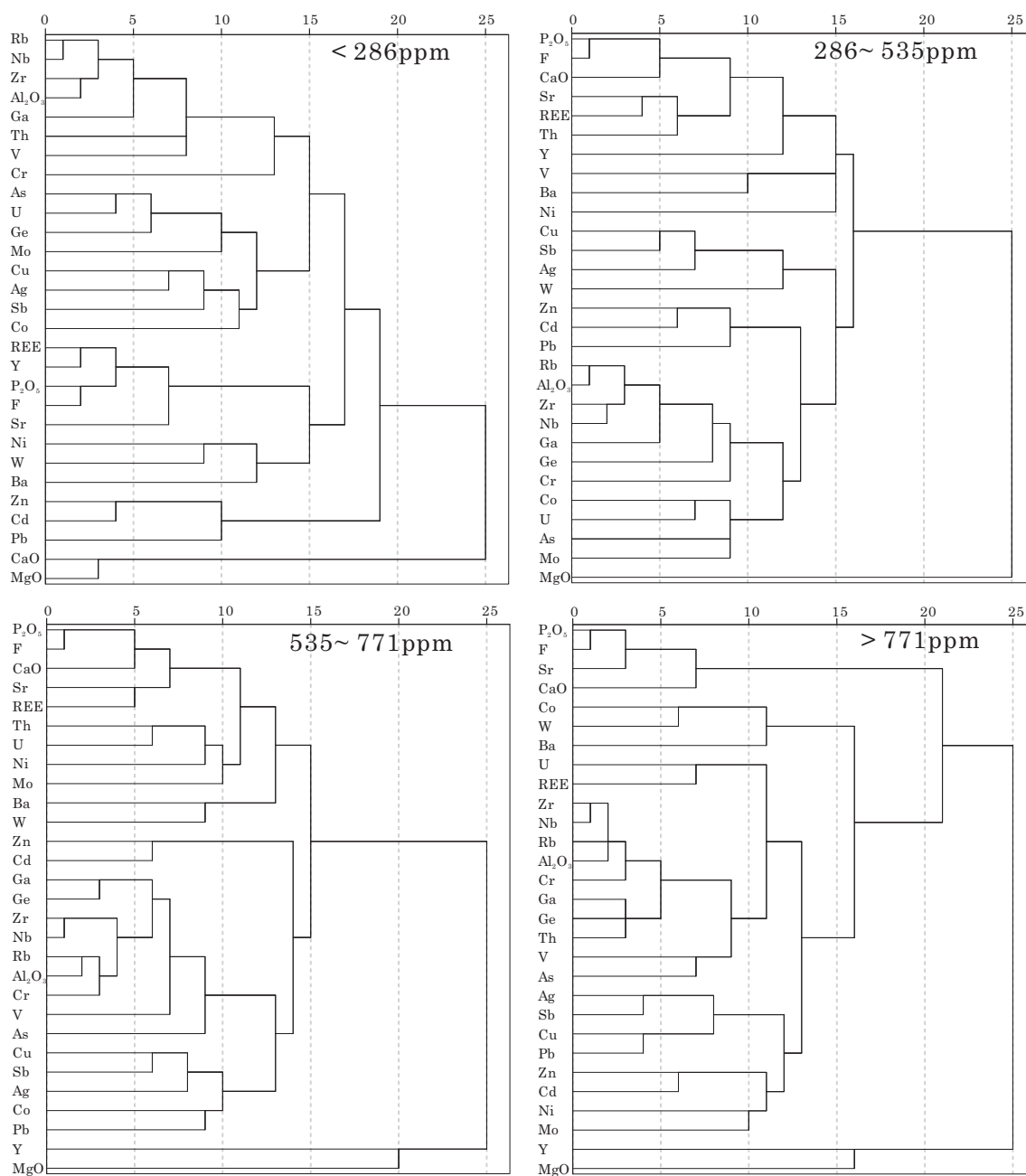


Fig. 8 Clustering analysis of Zhijin phosphorites

Table 3 KMO and Bartlett testing

Indicators		lower rare earth content (less than 535 ppm)	higher rare earth content (more than 535 ppm)
KMO number of samples relevant		0.752	0.841
Bartlett sphericity test	Approximate chi-square	2424.492	3015.855
	Free degree	406	406
	Significance	0.000	0.000

Table 4 Total variance interpretation of Zhijin phosphorites with lower rare earth content (less than 535 ppm)

Component	Initial characteristic values			Quadratic sum of extracted load			Quadratic sum of revolved load		
	Total	Variance (%)	Cumulation (%)	Total	Variance (%)	Cumulation (%)	Total	Variance (%)	Cumulation (%)
1	9.846	33.952	33.952	9.846	33.952	33.952	7.525	25.948	25.948
2	5.107	17.609	51.561	5.107	17.609	51.561	5.286	18.226	44.174
3	2.799	9.653	61.214	2.799	9.653	61.214	3.124	10.774	54.948
4	1.759	6.064	67.278	1.759	6.064	67.278	2.363	8.147	63.095
5	1.423	4.907	72.186	1.423	4.907	72.186	1.991	6.866	69.961
6	1.318	4.543	76.729	1.318	4.543	76.729	1.745	6.016	75.977
7	1.171	4.038	80.766	1.171	4.038	80.766	1.389	4.789	80.766
8	0.931	3.211	83.978						
9	0.749	2.583	86.560						
10	0.587	2.025	88.586						
11	0.492	1.698	90.283						
12	0.411	1.416	91.699						
13	0.368	1.269	92.968						
14	0.339	1.170	94.138						
15	0.287	0.990	95.128						
16	0.241	0.830	95.958						
17	0.208	0.717	96.675						
18	0.194	0.670	97.345						
19	0.176	0.607	97.952						
20	0.150	0.517	98.469						
21	0.111	0.383	98.851						
22	0.096	0.330	99.181						
23	0.077	0.265	99.445						
24	0.065	0.226	99.671						
25	0.035	0.121	99.792						
26	0.026	0.088	99.880						
27	0.015	0.053	99.933						
28	0.012	0.043	99.976						
29	0.007	0.024	100.000						

with a characteristic value greater than 1, and their values were the same as those of the initial eigenvalues. The variance interpretation of the rotation load factors represents the contribution value obtained by new factor variances obtained by the rotation of factors in the last column. Compared with the non-rotation factors, the variance contribution value of each common factor changes, but the final cumulative contribution rate of the variance remains unchanged.

Tables 6 and 7 show the matrices of component loads after rotation of the factor analyses data for Zhijin phosphorite samples with a lower REYs content (< 535 ppm) and higher REYs content (\geq 535 ppm), respectively. Using this matrix can help us better explain the meaning of the factors. Factor load is the correlation coefficient between a

factor and a variable. For a variable, the greater the absolute value of the load after rotation, the closer the relationship between the variable and its corresponding factor, and thus, the factor can also represent the variable. Therefore, during the study, the authors tagged the values that had an absolute value of the load greater than 0.5 in Tables 6 and 7 by roughening the texts of the values, and a summary is provided for the elements explained by each factor.

For Zhijin REYs-bearing phosphorite samples with a lower REYs content (total REYs < 535 ppm), elements correlated with factor 1 (F1) included REE, P_2O_5 , F, Sr, Y, Th, CaO, U, and Ge; elements correlated with factor 2 (F2) included Rb, Al_2O_3 , Nb, Zr, Ga, and Cr; elements correlated with factor 3 (F3) included Cu, Ag, Sb, and As;

Table 5 Total variance interpretation of Zhijin phosphorites with higher rare earth content (more than 535 ppm)

Component	Initial characteristic values			Quadratic sum of extracted load			Quadratic sum of revolved load		
	Total	Variance (%)	Cumulation (%)	Total	Variance (%)	Cumulation (%)	Total	Variance (%)	Cumulation (%)
1	13.204	45.532	45.532	13.204	45.532	45.532	8.519	29.374	29.374
2	4.249	14.652	60.184	4.249	14.652	60.184	5.694	19.634	49.009
3	2.981	10.280	70.464	2.981	10.280	70.464	3.281	11.315	60.323
4	1.590	5.483	75.947	1.590	5.483	75.947	3.017	10.403	70.726
5	1.177	4.059	80.006	1.177	4.059	80.006	2.471	8.521	79.247
6	1.090	3.757	83.763	1.090	3.757	83.763	1.310	4.517	83.763
7	0.929	3.202	86.965						
8	0.599	2.066	89.031						
9	0.457	1.577	90.608						
10	0.409	1.411	92.019						
11	0.367	1.266	93.285						
12	0.299	1.032	94.317						
13	0.260	0.896	95.213						
14	0.229	0.791	96.004						
15	0.213	0.734	96.738						
16	0.169	0.583	97.321						
17	0.150	0.519	97.840						
18	0.138	0.477	98.317						
19	0.104	0.358	98.675						
20	0.093	0.322	98.996						
21	0.080	0.275	99.272						
22	0.063	0.218	99.490						
23	0.047	0.164	99.654						
24	0.027	0.093	99.746						
25	0.025	0.085	99.831						
26	0.023	0.079	99.910						
27	0.014	0.048	99.958						
28	0.009	0.031	99.989						
29	0.003	0.011	100.000						

elements correlated with factor 4 (F4) included Zn, Cd, and Pb; elements correlated with factor 5 (F5) included As and Mo; elements correlated with factor 6 (F6) included Ni, W, and Ba; and the element correlated with factor 7 (F7) was V.

In REYs-bearing phosphorites with a low REYs content, the correlation coefficients between F1 and F, P_2O_5 , CaO, REE, and Y were 0.935, 0.939, 0.726, 0.959, and 0.899, respectively, which are values representative of a certain degree of REYs enrichment during the diagenesis of phosphorites. The correlation coefficient between F1 and MgO was -0.507 , which was weak relative to the other elements, so the concentration of dolomite was relatively high during the formation process of phosphorite. The correlation coefficients between F2 and Rb, Al_2O_3 , Nb, Zr,

and Ga were 0.928, 0.919, 0.904, 0.865, and 0.673, respectively, which are values considered to represent the addition process of terrestrial detrital flux. The correlation coefficient between F2 and MgO was -0.437 , which represents the leaching of dolomite during the addition of terrestrial detrital flux. However, the correlation was relatively weak (the absolute value was less than 0.5), which indicates that the addition from the terrestrial detrital flux was not strong. Because of the high concentration of dolomite during the diagenesis, as well as the additional weak terrestrial detrital flux, the concentration of apatite in phosphorite was relatively low, so the content of REYs was relatively low.

For Zhijin REYs-bearing phosphorites with a high REYs content (total REYs ≥ 535 ppm), the elements correlated

Table 6 Component load matrix after rotation of Zhijin phosphorites with low rare earth content (total REY content less than 535 ppm)

elements	F1	F2	F3	F4	F5	F6	F7
REE	0.959	0.070	0.053	– 0.058	– 0.024	0.066	– 0.066
P ₂ O ₅	0.939	– 0.005	0.119	– 0.051	0.061	0.068	0.198
F	0.935	– 0.004	0.144	– 0.067	0.050	0.091	0.168
Sr	0.915	0.061	0.144	– 0.097	– 0.083	0.157	– 0.078
Y	0.899	0.089	– 0.008	– 0.124	0.130	– 0.097	– 0.070
Th	0.801	0.362	0.179	– 0.174	– 0.025	0.080	– 0.114
CaO	0.726	– 0.422	– 0.073	– 0.132	– 0.209	0.075	0.322
U	0.640	0.255	0.235	0.022	0.475	– 0.031	0.206
Ge	0.591	0.410	0.284	0.107	0.342	– 0.022	– 0.291
MgO	– 0.507	– 0.437	– 0.371	– 0.049	– 0.395	– 0.017	0.043
Rb	– 0.072	0.928	0.016	0.085	0.060	0.139	– 0.057
Al ₂ O ₃	– 0.001	0.919	0.138	0.182	0.118	0.055	0.016
Nb	0.069	0.904	0.005	0.026	0.082	0.089	0.131
Zr	0.339	0.865	0.075	0.000	0.023	0.071	0.095
Ga	0.601	0.673	0.174	0.106	0.059	0.113	– 0.052
Cr	– 0.034	0.534	– 0.141	0.121	0.298	– 0.034	0.452
Cu	0.170	0.012	0.852	– 0.128	0.066	0.151	0.001
Ag	0.073	– 0.069	0.833	0.168	0.110	– 0.212	0.155
Sb	0.276	0.232	0.716	0.082	0.144	0.279	– 0.155
As	0.175	0.187	0.581	0.128	0.578	– 0.234	– 0.114
Co	– 0.030	0.334	0.485	0.422	0.130	0.147	0.416
Zn	– 0.213	0.152	– 0.043	0.847	0.125	0.084	0.085
Cd	– 0.232	0.007	– 0.086	0.809	0.024	– 0.163	– 0.148
Pb	0.076	0.108	0.280	0.734	– 0.009	– 0.071	0.021
Mo	– 0.082	0.107	0.196	0.083	0.819	0.055	0.043
Ni	0.025	0.068	0.044	– 0.075	– 0.126	0.795	0.123
W	0.123	0.254	0.075	– 0.015	0.134	0.673	– 0.410
Ba	0.353	0.130	– 0.068	– 0.054	0.435	0.527	0.198
V	0.373	0.434	0.191	– 0.159	0.046	0.062	0.579

with factor 1 (F1) included Rb, Al₂O₃, Nb, Zr, Ga, Cr, Th, Ge, V, and MgO; the elements correlated with factor 2 (F2) included MgO, P₂O₅, F, Sr, CaO, REE, and U, the elements correlated with factor 3 (F3) included Zn, Cd, Mo, Ni, and As; the elements correlated with factor 4 (F4) included W, Co, Ba, and Cu; the elements correlated with factor 5 (F5) included Cu, Ag, Pb, and Sb; and the element correlated with factor 6 (F6) was Y.

For Zhijin phosphorite with a high REYs content, the correlation coefficients between F1 and Rb, Al₂O₃, Nb, Zr, Ga, Cr, Th, Ge, V, and MgO were 0.912, 0.911, 0.907, 0.894, 0.854, 0.865, 0.743, 0.740, 0.724, and – 0.665, respectively, which are values considered to represent the addition from the terrestrial detrital flux. The correlation coefficient between F1 and MgO was – 0.665, which indicates that the correlation was strong and further demonstrates that the addition from the continental detrital flux was stronger relative to phosphorites with a low REYs content; this led to more leaching of dolomite. The

correlation coefficients between F2 and MgO, P₂O₅, F, Sr, CaO, REE, and U were – 0.584, 0.971, 0.964, 0.849, 0.823, 0.800, and 0.582, respectively, and it is thought that REE enrichment occurred during the diagenesis of phosphorite. The correlation coefficient between F2 and MgO was – 0.584, and the correlation was strong; hence, the concentration of dolomite was relatively low during the formation process of phosphorites. Because of the low concentration of dolomite during the diagenesis process of phosphorite and the relatively strong addition process of continental detrital flux, the concentration of apatite in the phosphorite is relatively high, and thus, the REYs are more enriched. Nevertheless, for phosphorites with a high REYs content, the correlation between F6 and Y was 0.897, Y enrichment was correlated with F6; while REEs enrichment was correlated with F2 (the correlation between F2 and REEs was 0.800). This indicates that Y enrichment processes are different from other REEs.

Table 7 Component load matrix after rotation of Zhijin phosphorites with high rare earth content (total REY content more than 535 ppm)

Elements	F1	F2	F3	F4	F5	F6
Rb	0.912	− 0.129	0.211	0.095	0.129	0.082
Al ₂ O ₃	0.911	− 0.048	0.138	0.006	0.132	0.008
Nb	0.907	0.127	0.162	0.087	0.183	0.042
Zr	0.894	0.219	0.108	0.078	0.223	0.035
Cr	0.865	0.008	0.181	− 0.021	0.229	0.212
Ga	0.854	0.366	0.064	0.213	0.178	− 0.094
Th	0.743	0.491	0.137	0.142	0.122	− 0.148
Ge	0.740	0.452	0.120	0.167	0.180	− 0.067
V	0.724	0.089	0.432	0.245	− 0.158	0.185
MgO	− 0.665	− 0.584	− 0.088	− 0.115	− 0.271	− 0.035
P ₂ O ₅	0.131	0.971	0.010	0.087	0.045	0.021
F	0.087	0.964	0.016	0.132	0.056	0.022
Sr	0.253	0.849	0.059	0.201	0.161	0.045
CaO	− 0.437	0.823	− 0.073	0.012	− 0.155	0.017
REE	0.421	0.800	0.056	0.075	0.174	0.042
U	0.428	0.582	0.446	0.299	− 0.011	0.152
Zn	0.135	− 0.054	0.854	0.188	0.202	0.158
Cd	0.136	− 0.144	0.698	0.094	0.159	0.185
Mo	0.277	0.156	0.663	0.206	0.119	− 0.179
Ni	0.157	0.222	0.631	0.455	− 0.037	− 0.197
As	0.519	0.310	0.546	− 0.105	0.273	0.185
W	− 0.031	0.096	0.195	0.870	0.037	0.114
Co	0.106	0.045	0.244	0.751	0.268	− 0.055
Ba	0.214	0.398	0.057	0.719	0.077	0.015
Ag	0.381	0.154	0.138	0.029	0.821	− 0.133
Pb	0.194	0.071	0.321	0.371	0.676	0.237
Sb	0.503	0.086	0.190	0.294	0.604	− 0.255
Cu	0.369	0.153	0.279	0.541	0.554	0.178
Y	0.117	0.113	0.123	0.075	− 0.026	0.897

The results of the cluster analysis suggested that, for phosphorites with a low REYs content (total REYs < 535 ppm), there was a good correlation between REEs, Y, and P₂O₅; for phosphorites with a high REYs content (total REYs ≥ 535 ppm), there also was a good correlation between REEs and P₂O₅, but there was no correlation between Y and P₂O₅. Moreover, the factor analysis also showed that Y was enriched congruently with REEs during the formation of phosphorites with a low REYs content (total REYs < 535 ppm); however, for the phosphorites with a high REYs content (total REYs ≥ 535 ppm), Y showed an inconsistent enrichment process compared with the other REEs. As a consequence, it may be concluded that superposition and enrichment activities were occurring during the accumulation of REYs in the Zhijin phosphorites, that is, the accumulation of REYs could have been caused by diagenesis, and the addition of continental detrital flux resulted in the leaching of MgO in dolomite, which in turn led to the enrichment of REYs in

phosphorites. The inconsistent enrichment processes of REYs may be indicative of more complex Y sources than previously proposed.

7 Discussion

7.1 Identification of the original deposition parameters

From material sources to sedimentary mineralization, material-forming minerals must go through a series of processes, including pre-sedimentary source material release, separation, transport, accumulation, sedimentary diagenesis, and reworking of post-diagenesis (Ye 1963). Presently, it is a complex problem to distinguish the pre- and post-diagenesis enrichment of materials. The identifications for original deposition parameters can be used to

solve this problem. The identifications involve both REEs parameters and major element parameters.

7.1.1 Identification of the REEs parameters

The identification of the REEs parameters focused on two aspects, i.e., the Ce anomaly and the $\text{Er}_\text{N}/\text{Lu}_\text{N}$ ratios of the distribution patterns.

- (1) Ce anomaly. The distribution pattern of REEs has characteristic Ce anomalies, which may be from two aspects, that is, the judgment of a real Ce anomaly and the correlations between the Ce anomaly and parameters correlated with REEs.

First, we discuss the real Ce anomaly. Shields and Stille (2001) believe that, relative to Pr_N or Nd_N , some phosphorites will show greater La_N enrichment, which results in uncertainty in the calculation of Ce anomalies. Bau and Dulski (1996) think the problem can be solved by the equation $\text{Pr}/\text{Pr}^* = 2 \text{Pr}_\text{N}/(\text{Ce}_\text{N} + \text{Nd}_\text{N})$. Since no chemical factor will result in Nd or Pr anomalies, the existence of real Ce anomalies will result in values of Pr/Pr^* that are not less than 1. Based on the relationship between the Ce anomaly (δCe , calculated here by the formula $\delta\text{Ce} = \text{Ce}/\text{Ce}^* = \text{Ce}_\text{N}/(0.5\text{La}_\text{N} + 0.5\text{Pr}_\text{N})$ (Bau and Dulski 1996) and the Pr/Pr^* value, Bau and Dulski (1996) divided the Ce and La anomalies into five situations (Fig. 8). According to Bau and Dulski (1996), we investigated the relationship between δCe and Pr/Pr^* in the Zhijin phosphorites and found that the Ce anomaly of Zhijin phosphorites is located

in the IIIb domain, which belongs to the real Ce anomaly range (Fig. 9); thus, the real Ce anomalies indicate that the phosphorites were formed under oxidizing conditions.

Second, we discuss the correlations between the Ce anomaly and REEs parameters. Shields and Stille (2001) believe that, during the reworking of post-diagenesis, with the enrichment of REYs, the deviation of the REYs distribution pattern between seawater and phosphorites will increase, and this will keep the REYs distribution patterns of phosphorites away from the influence of oxidized seawater. As a consequence, the phosphorites affected by post-diagenetic reworking will show a good correlation between δCe and the REYs content, as well as δEu and $\text{Dy}_\text{N}/\text{Sm}_\text{N}$. However, for original phosphorites, the correlation between δCe and REYs will be poor. Morad and Felitsyn (2001) proposed that if $(\text{La}/\text{Sm})_\text{N}$ does not correlate with δCe and $(\text{La}/\text{Sm})_\text{N}$ is greater than 0.35, the Ce anomalies in apatite represent the original signature of seawater.

For Zhijin phosphorites, there were no correlations detected between δCe and $\sum\text{REY}$, δCe and $\text{Dy}_\text{N}/\text{Sm}_\text{N}$, and δCe and $(\text{La}/\text{Sm})_\text{N}$ (Fig. 10), and the $(\text{La}/\text{Sm})_\text{N}$ values were above 0.5 (Fig. 10D), thus indicating that the Ce anomalies of Zhijin phosphorites were the original features of seawater, and the whole REYs series was only slightly affected by post-diagenetic reworking.

- (2) The $\text{Er}_\text{N}/\text{Lu}_\text{N}$ ratios of the REYs distribution pattern. Higher $\text{Er}_\text{N}/\text{Lu}_\text{N}$ ratios result from HREEs depletion. Shields and Stille (2001) studied Meishucun and Maidiping phosphorites in South China, which belong to the same Early Cambrian epoch, and the results showed that the Meishucun phosphorites exhibited consistent HREEs depletion from Er to Lu with higher $\text{Er}_\text{N}/\text{Lu}_\text{N}$ ratios (1.73–3.37), while the Maidiping phosphorites had lower $\text{Er}_\text{N}/\text{Lu}_\text{N}$ ratios (1.67–1.72). Shields and Stille (2001) believe that the REEs content of the Maidiping phosphorites with lower $\text{Er}_\text{N}/\text{Lu}_\text{N}$ ratios may have originated from late weathering rather than the rare earth exchange of early diagenesis, while those of Meishucun phosphorites with higher $\text{Er}_\text{N}/\text{Lu}_\text{N}$ ratios may have originated from the rare earth exchange of early diagenesis. The $\text{Er}_\text{N}/\text{Lu}_\text{N}$ ratios of Zhijin phosphorites were 1.26–2.59, with an average of 1.99 and a median of 1.97 (Fig. 11A), which are values similar to those of Meishucun phosphorites, thus indicating that REYs of Zhijin phosphorites originated from the rare earth exchange of early diagenesis, and the influence of post-diagenetic reworking was very small.

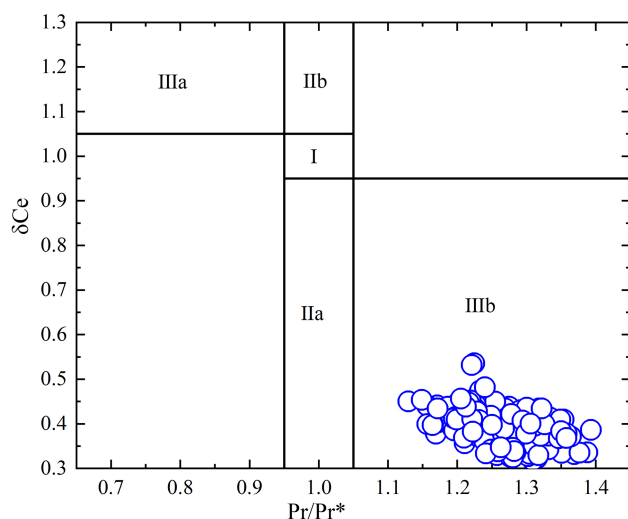


Fig. 9 δCe - Pr/Pr^* map of Zhijin phosphorites, which domain partition according to Bau and Dulski (1996). Domain **I** no Ce anomalies and no La anomalies. Domain **IIa** positive La anomalies, no Ce anomalies. Domain **IIIb** negative La anomalies, no Ce anomalies. Domain **IIIa** positive Ce anomalies. Domain **IIIb** negative Ce anomalies

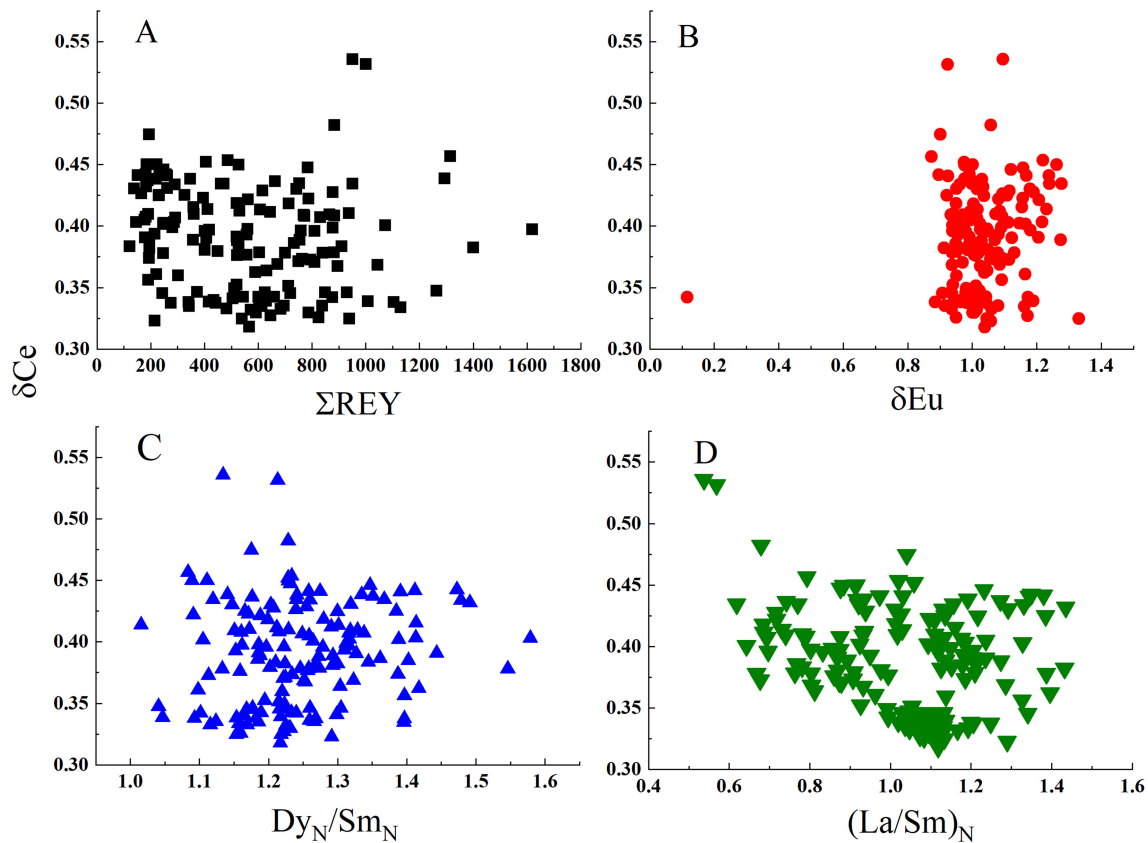


Fig. 10 The scatter plots of δCe vs. ΣREY (A), δCe vs. δEu (B), δCe vs. $\text{Dy}_\text{N}/\text{Sm}_\text{N}$ (C) and δCe vs. $(\text{La}/\text{Sm})_\text{N}$ (D)

7.1.2 Identification of the major element parameters

Identification of the major element parameters principally involved MgO (%), $\text{CaO}/\text{P}_2\text{O}_5$, and $(\text{CaO} + \text{MgO})/\text{P}_2\text{O}_5$, which are indicators that can be used to distinguish reworked phosphorites from original phosphorites. Ge (1994) argues that MgO (%) values less than 1.46, $\text{CaO}/\text{P}_2\text{O}_5$ values less than 1.5, and $(\text{CaO} + \text{MgO})/\text{P}_2\text{O}_5$ values less than 1.54 are the proxies of weathered phosphorites; otherwise, the data are indicators of original phosphorites. The values of MgO (%), $\text{CaO}/\text{P}_2\text{O}_5$, and $(\text{CaO} + \text{MgO})/\text{P}_2\text{O}_5$ in Zhijin phosphorites indicated that the phosphorites have original properties (Fig. 11B, C, D).

In general, Zhijin phosphorites have the signature of original phosphorites in terms of either the parameters of REYs or the parameters of major elements. Additionally, the influence of post-diagenetic reworking on the distribution patterns of REYs is very small. Therefore, the conclusion can be reached that the REYs in the Zhijin phosphorites came from original sources.

7.2 Y sources

7.2.1 Effect of seafloor hydrothermal activity

Eu anomalies. Positive Eu anomalies can be indicative of a hydrothermal source for REYs and are usually used as indicators for a reductive seafloor hydrothermal supply (Douville et al. 1999; Yi et al. 1995). The REYs distribution pattern of the modern Mid-Ocean Ridge is typical of positive Eu anomalies (Fig. 13), but its REYs content is low, with REYs content values within the range of 470.06–1630.21 uppm (median of 1019.79 uppm, mean of 1040.02 uppm) and Y content values within the range of 55.84–158.70 uppm (median of 97.09 uppm, mean of 103.88 uppm) (Table 8, data are from Bau and Dulski 1999). Despite the low content of Y, a steady flux of seafloor hydrothermal fluids directly provided a source for Y in the Mid-Ocean Ridge.

The Eu anomalies of Zhijin phosphorite indicate that there was no direct supply source of reductive submarine hydrothermal fluids for Y. The values of δEu in the Early Cambrian Zhijin phosphorites were between 0.03–1.25, but usually, around 1.0, as shown in Table 1 and Fig. 12A. Since there generally was no Eu anomaly in the Early Cambrian Zhijin phosphorites, and there was no correlation

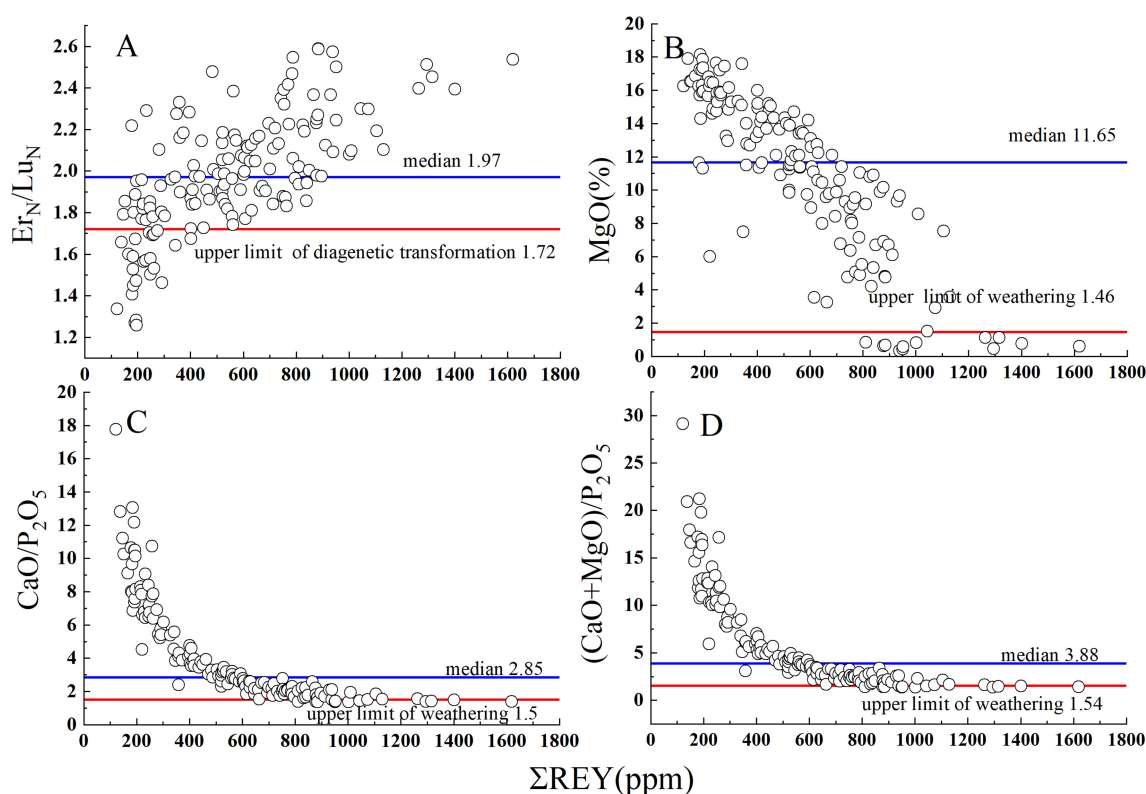


Fig. 11 The scatter diagrams of Er_N/Lu_N vs. ΣREY (A), $\text{MgO}(\%)$ vs. ΣREY (B), $\text{CaO}/\text{P}_2\text{O}_5$ vs. ΣREY (C) and $(\text{CaO} + \text{MgO})/\text{P}_2\text{O}_5$ vs. ΣREY (D). The upper limit of weathering according to Ge(1994)

Table 8 REY values of Mid-Ocean Ridges (data from Bau and Dulski 1999)

Elements	Atomic weight	HT-1c		HT-5		HT-20	
		pmol/kg	uppm	pmol/kg	uppm	pmol/kg	uppm
La	138.9	545	75.70	812.00	112.79	1585.00	220.16
Ce	140.1	1258	176.25	2082.00	291.69	1900.00	266.19
Pr	140.9	130	18.32	349.00	49.17	262.00	36.92
Nd	144.2	490	70.66	1512.00	218.03	1011.00	145.79
Sm	150.4	102	15.34	374.00	56.25	219.00	32.94
Eu	152	156	23.71	4152.00	631.10	1021.00	155.19
Gd	157.3	87.7	13.80	303.00	47.66	176.00	27.68
Tb	158.9	10.1	1.60	38.20	6.07	22.20	3.53
Dy	162.5	55.4	9.00	186.00	30.23	104.00	16.90
Y	88.91	628	55.84	1785.00	158.70	1092.00	97.09
Ho	164.9	9.72	1.60	30.80	5.08	19.10	3.15
Er	167.3	25.3	4.23	75.00	12.55	45.30	7.58
Tm	168.9	3.1	0.52	9.01	1.52	5.66	0.96
Yb	173	17.6	3.04	47.20	8.17	29.00	5.02
Lu	175	2.53	0.44	6.86	1.20	4.05	0.71
ΣREY			470.06		1630.21		1019.79

between δEu and Y (Table 1 and Fig. 12A), it can be inferred that there was no direct supply of reductive seafloor hydrothermal fluids to Y.

Representative elements of seafloor hydrothermal activity and ratio of seafloor hydrothermal elements. The element contents of Ag, As, and Sb and the element ratio of $\text{Al}/(\text{Al} + \text{Fe} + \text{Mn})$ can be used as indicators for seafloor

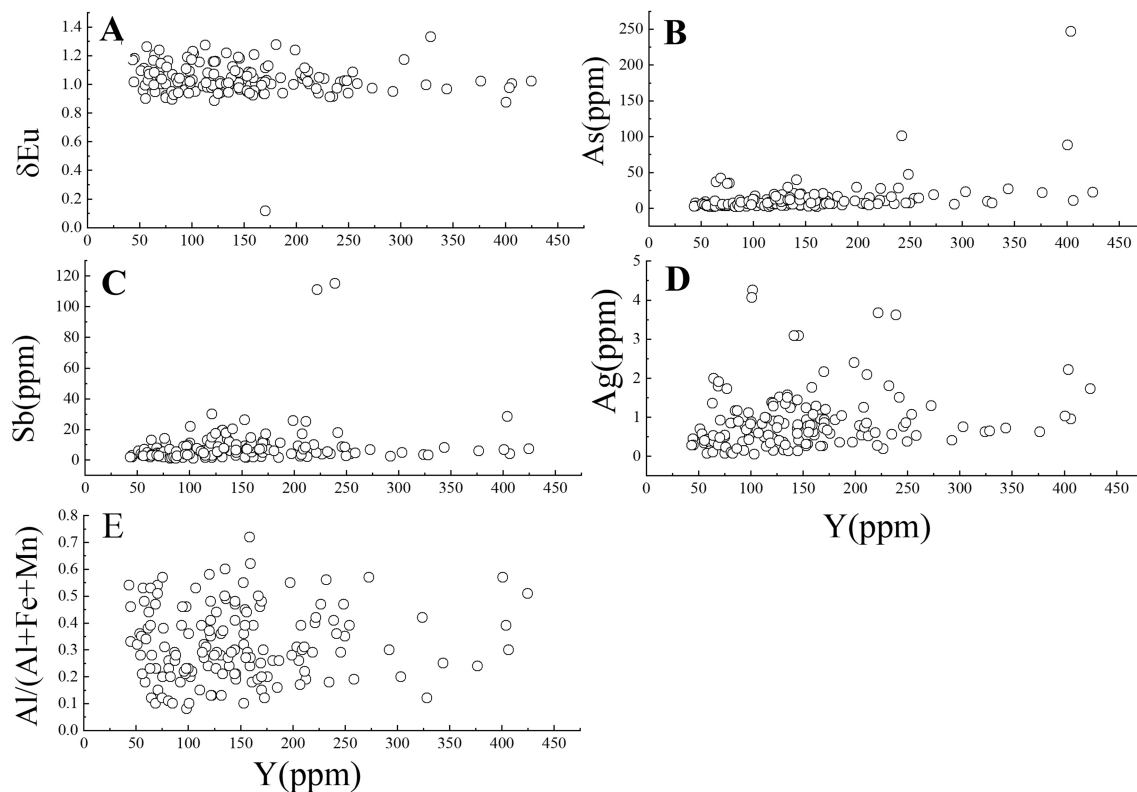


Fig. 12 Scattered plots of the relationship between Y and δEu , the contents and ratios of seafloor hydrothermal elements of Zhijin bearing-rare earthphosphorites. **A** Y vs. δEu ; **B** Y vs. As; **C** Y vs. Sb; **D** Y vs. Ag; **E** Y vs. $\text{Al}/(\text{Al}+\text{Fe}+\text{Mn})$

hydrothermal deposition (Hekinian and Fouquet 1985; Marchig et al. 1982; Adachi et al. 1986). The Ag and As contents of seafloor hydrothermal sediments in modern Pacific Mid-Ocean Ridge areas are high, with an Ag content that ranges from 5 to 186 ppm (average of 37 ppm) and As content that ranges from 45 to 1253 ppm (average of 252 ppm) (Hekinian and Fouquet 1985). Marchig et al. (1982) suggested that the contents of As and Sb can be used to distinguish seafloor hydrothermal sedimentary activity from normal sedimentary activity. The contents of As and Sb for seafloor hydrothermal sedimentary are higher, and the average values of As and Sb contents are more than 100 ppm and 7 ppm, respectively. In contrast, those of normal deposition is lower, and the average values of As and Sb contents are 10 ppm and 2–3 ppm, respectively (Marchig et al. 1982). An $\text{Al}/(\text{Al} + \text{Fe} + \text{Mn})$ ratio, as a percentage of mass, can also be used as a proxy of seafloor hydrothermal sediments. A larger $\text{Al}/(\text{Al} + \text{Fe} + \text{Mn})$ ratio is indicative of fewer seafloor hydrothermal deposits (Adachi et al. 1986).

Representative elements of the hydrothermal activity of Zhijin phosphorites indicated that submarine hydrothermal fluids did not directly supply the Y source. For the Early Cambrian Zhijin phosphorites, the Ag contents (ppm) changed from 0.052 to 4.25 with a median of 0.707 and an

average of 0.884, the As contents (ppm) changed from 1.89 to 247 with a median of 7.30 and an average of 12.89, the Sb contents (ppm) changed from 0.92 to 115 with a median of 5.78 and an average of 8.70, the $\text{Al}/(\text{Al} + \text{Fe} + \text{Mn})$ ratios changed from 0.08 to 0.72 with a median of 0.30 and an average of 0.32. This indicates that, when taking into account either the contents of representative elements Ag, As, and Sb of seafloor hydrothermal activity or the ratio $\text{Al}/(\text{Al} + \text{Fe} + \text{Mn})$ of seafloor hydrothermal elements, the Early Cambrian Zhijin phosphorite displays normal deposition characteristics rather than seafloor hydrothermal deposition characteristics. As far as both the contents of seafloor hydrothermal elements and the ratios of seafloor hydrothermal element are concerned, the values were not correlated with Y (Fig. 12), which indicates that the seafloor hydrothermal supply had little effect on the source supply of Early Cambrian Zhijin phosphorites, and the seafloor hydrothermal fluids were not a direct supply source for Y.

7.2.2 Oxidative seawater as a primary source

The oxidation background is important for understanding the source of the metallogenic material. The abundance of small-shell fossils in the Early Cambrian Zhijin

phosphorites is reflective of the oxidation background of the oceans at that time. Zhang and Cui (2016) proposed that in each historical geological period, there was a minimum demand for oxygen to maintain the survival of organisms. During the Ediacara–Cambrian transition, the anoxic ocean shrank and oxygen levels continued to rise, and the oxygen level, which maintained biodiversity, was at least 25% of the present atmospheric level (Zhang and Cui 2016). The oxidation background not only was important for oxygen and nutrient inputs (such as phosphorus enrichment) but also brought about an important material basis for diagenetic mineralization at the same time when the Cambrian biological explosion was triggered.

The characteristic REYs data of oxidized seawater, terrestrial phosphorites, and Mid-Ocean Ridge and Zhijin phosphorites are shown in Table 9. Among them, the sample ZKX001-648 is Zhijin phosphorite, which is negative Ce anomaly and positive Y anomaly, no Eu anomaly or weak positive Eu anomaly (data from this study). M79/11 is an oxidized seawater sample (data from McArthur and Walsh 1984), which has an obvious negative Ce anomaly. NY-BC-SIM3 is a terrigenous source sample (data from McArthur and Walsh 1984), which has the characteristics of MREEs enrichment and HREEs depletion. And HT-5 is a Mid-Ocean Ridge sample (data from Bau and Dulski 1999), which is typical of positive Eu anomaly.

According to Table 9, we plotted the charts of REYs distribution patterns of oxidized seawater, terrestrial

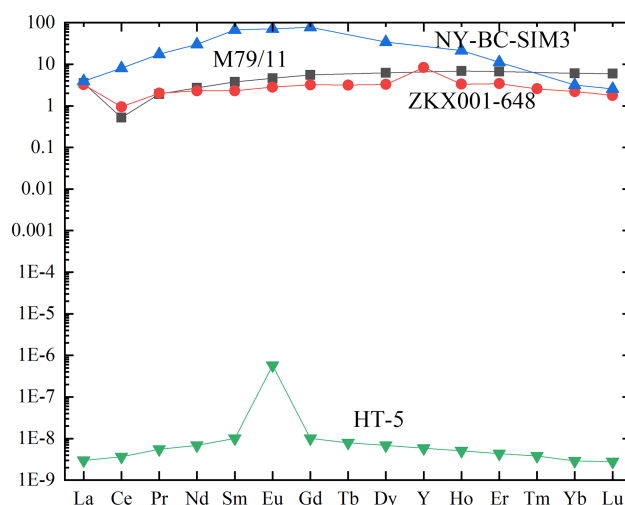


Fig. 13 Comparison of patterns of rare earth distribution. The sample ZKX001-648 is Zhijin phosphorite and its data comes from this study. The M79/11 belongs to the oxidized seawater REY model, NY-BC-SIM3 belongs to the land-based REY model, data from the McARTHUR and WALSH (1984). HT-5 mid-ocean ridge REY model, data from the Bau and Dulski(1999)

phosphorites, and Mid-Ocean Ridge and Zhijin phosphorites (Fig. 13). As shown in Fig. 13, the typical rare earth distribution pattern of oxidized seawater showed a negative Ce anomaly, no obvious Eu anomaly, and LREEs depletion relative to HREEs (curve M79/11 in Fig. 13, data according to McArthur and Walsh 1984). Meanwhile, some terrestrial phosphorites (curve NY-BC-SIM3 in Fig. 13, data according to McArthur and Walsh 1984) and Mid-Ocean Ridge phosphorites (curve HT-5 in Fig. 13, data according to Bau and Dulski 1999) showed distribution patterns of rare earth with HREEs depletion.

The REYs distribution pattern of Zhijin phosphorites indicated that the Y may have originated from seawater as well as from the addition of terrestrial materials. The REYs distribution patterns in Early Cambrian Zhijin phosphorites were characterized by a negative Ce anomaly, no Eu anomaly, positive Y anomaly, MREEs enrichment, and HREEs depletion (curve ZKX001-648 in Fig. 13). Compared to the REYs distribution pattern of the seawater-type, terrestrial materials-type, and Mid-Ocean Ridge-type, the REYs distribution pattern of Early Cambrian Zhijin phosphorite was similar to the characteristics of oxidative seawater in the La-Er section, but the Tm-Lu segment was similar to the characteristics of terrestrial materials (Fig. 13). Because Zhijin phosphorite is of an original character and had no seafloor hydrothermal supply, the REYs may have come principally from seawater, but there may have been the superimposition of terrestrial sources. That is, the source was possibly a mixture of seawater and terrestrial sources.

Table 9 REY characteristic data of oxidized seawater, continental phosphorite, Mid-Ocean Ridge and Zhijin phosphorite (ppm)

Samples	M79/11	ZKX001-648	NY-BC-SIM3	HT-5
La	3.53	3.22	3.93	0.000002968
Ce	0.52	0.95	8.04	0.000003646
Pr	1.93	2.02	17.55	0.000005525
Nd	2.72	2.31	29.92	0.000006813
Sm	3.78	2.31	67.57	0.000010045
Eu	4.63	2.82	71.30	0.000573731
Gd	5.58	3.21	77.25	0.000010141
Tb		3.17		0.000001084
Dy	6.20	3.27	34.19	0.000006869
Y		8.40		0.000005878
Ho	6.86	3.33	21.19	0.000005079
Er	6.67	3.41	11.23	0.000004327
Tm		2.57		0.000003804
Yb	6.03	2.21	3.19	0.000002916
Lu	6.00	1.79	2.54	0.000002792

7.2.3 Terrestrial source

The Y/Ho ratios of Early Cambrian Zhijin phosphorites also demonstrate that the REYs may have come from a mixture of seawater and terrestrial sources. Y/Ho is an important indicator for distinguishing terrigenous and seawater origins (Abedini and Calagari 2017; Bau et al. 1997). The Y/Ho values of 28 and 60 are REYs features of terrigenous and seawater origins, respectively (Abedini and Calagari 2017; Bau et al. 1997; Bau and Dulski 1999; Nozaki et al. 1997). The Y/Ho values of the Zhijin phosphorites ranged from 72.18 to 15.82, thus spanning the scopes of terrestrial sources and seawater characteristics. The Y/Ho (median) varied regularly as the total REYs content varied regularly from low to high. That is, when the total REYs content was less than 535 ppm, the median Y/Ho value was 43.60 and the Y/Ho values converged, whereas when the total REYs content was more than 535 ppm, the median Y/Ho value was 30.41 and the Y/Ho values were diffuse. The trend of Y/Ho changes with the total REYs content showed that as the total REYs content increased from low to high, the Y/Ho ratio gradually decreased from the values approximate to the seawater toward the values approximate to the terrigenous source (Fig. 14A). This indicates that when the total REYs content was low, the sedimentary environment was similar to the ocean, the source for REYs was approximate to seawater; however, when the total REYs content was high, the sedimentary environment was similar to the terrestrial environment, and the source for REYs elements was extensive but approximate generally to a terrestrial origin.

The Er/Nd values of Early Cambrian Zhijin phosphorites indicated that the origin for terrestrial clastic material may have played an important role in Y enrichment when

the REYs content was high. Mao et al. (2015) believed that the Zhijin phosphorite is generally controlled by the surface of unconformity of old karst formed by ancient weathering. Ancient weathering not only resulted in the base of the phosphorite bed but also played a role in the deposition process of phosphorite that may have provided the origins for Y enrichment. The Er/Nd ratio of normal seawater is approximately 0.27, and the detritus can make the Nd preferentially concentrated relative to Er, thus reducing the Er/Nd value to less than 0.11 (Abedini and Calagari 2017). The Er/Nd values of Zhijin phosphorites ranged from 0.087 to 0.14 (median of 0.11). When the total REYs content was less than 286 ppm, the Er/Nd values ranged from 0.089 to 0.146 (median of 0.125). When the total REYs content changed from 286 to 535 ppm, the Er/Nd values ranged from 0.096 to 0.141 (median of 0.112). When the total REYs content changed from 535 to 771 ppm, the Er/Nd values ranged from 0.096 to 0.128 (median of 0.110). When the total REYs content was more than 771 ppm, the Er/Nd values ranged from 0.087 to 0.128 (median of 0.103) (Fig. 15). The ratios of Er/Nd confirmed the terrestrial detrital origin for REYs. Usually, the correlation between Er/Nd and Y was weak, but when the total REYs content was more than 771 ppm, Er/Nd and Y showed a stronger correlation ($R = -0.545$) (Fig. 15D), thus indicating that the origin for terrestrial clastic material may have played an important role in the enrichment of terrestrial materials when the REYs content was high.

7.2.4 Offshore distance and water depth

Tian and Zhang (2016) believe that Mn/Ti and MnO₂ concentrations can represent the offshore distance and water depth, respectively. Specifically, it has been

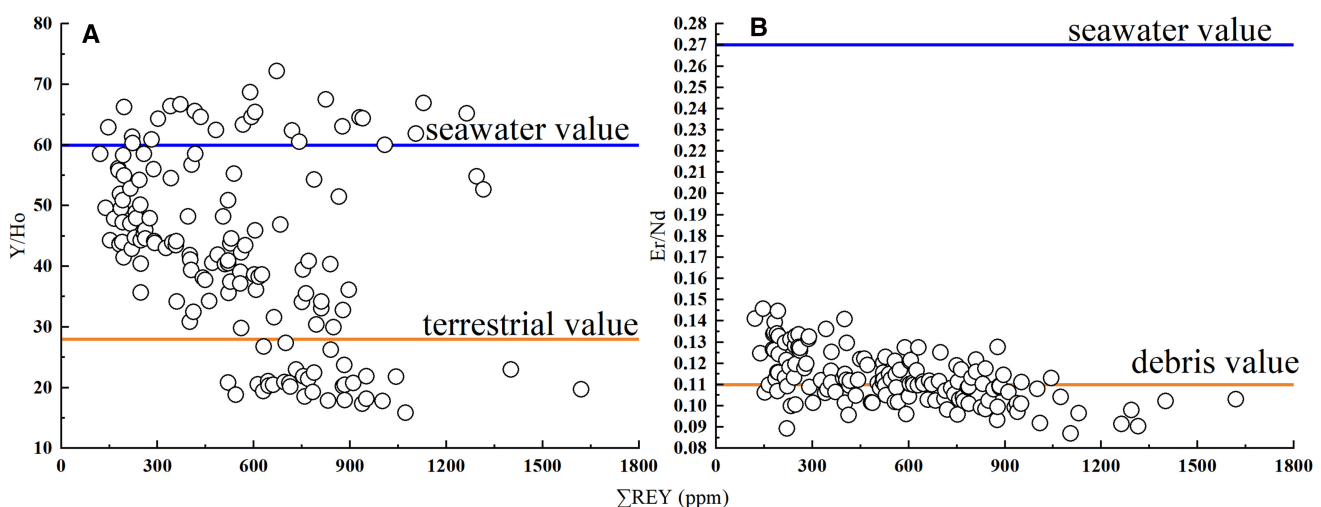
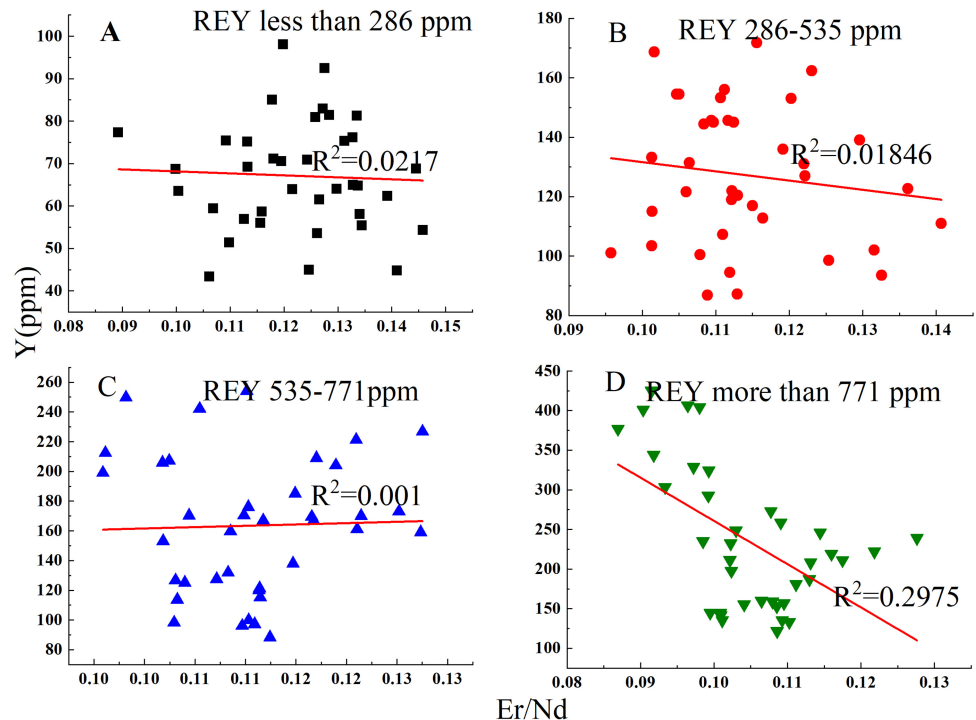


Fig. 14 Scattered plots of Y/Ho, Er/Nd vs. Σ REY in Zhijin phosphorites. **A** Y/Ho vs. Σ REY. **B** Er/Nd vs. Σ REY. Reference data for seawater, land and debris come from Abedini and Calagari (2017)

Fig. 15 Scatter plots of Y vs. Er/Nd in Zhijin phosphorites with different total REY content



suggested that offshore distances are associated with Mn/Ti values, and seawater depths are associated with MnO₂ concentrations (Tian and Zhang 2016). The Mn/Ti of 100 m offshore is equal to 0.1. From lakeside to deep water, the MnO₂ concentration will increase from 0.00094% to 0.051%. The Mn/Ti values of the Zhijin phosphorite samples were between 0.0527–34.76 (median of 5.983), which denotes a median offshore distance of approximately 6 km. MnO₂ concentrations of the Zhijin phosphorite samples were greater than 0.01 (median of 0.1100 and average of 0.1453), which suggests that the overall environment belonged to a deep-water body. The values of Mn/Ti and MnO₂ were negatively correlated with

Y (Fig. 16), which suggests that the greater the offshore distance and/or the deeper the seawater, the less Y enrichment occurred. In contrast, the smaller the offshore distance and/or the shallower the seawater, the more Y enrichment occurred. Additionally, smaller offshore distances and shallower seawater were more favorable for the transport of terrigenous materials involving Y into marine sediments, which is suggestive of the contribution of terrestrial detrital flux to Y. This also confirms the foregoing conclusions that some Y came from the source of terrigenous detrital flux as discussed with the Er/Nd results.

The free property of Y allows it to enrich easily during the process of phosphorite formation. As far as the deposition process is concerned, REYs can be absorbed from either seawater or occluded in associated biological fragments and/or other clastic fluxes (McArthur and Walsh 1984) followed by reactivation into pore water during the formation of phosphorites. However, REYs must go through the processes of weathering, activation, transport, and placement before the accumulation and mineralization from the parent rock into the phosphorites. The addition of a pre-diagenesis terrigenous detrital flux is a major geological driving factor in the sedimentary diagenesis process. McArthur and Walsh (1984) proposed that weathering will give priority to the removal of LREEs. Due to the preferential removal of LREEs, weathering may result in HREEs enrichment and LREEs depletion in debris in the parent rock area. In contrast, for the material components transported to seawater, the situation is reversed,

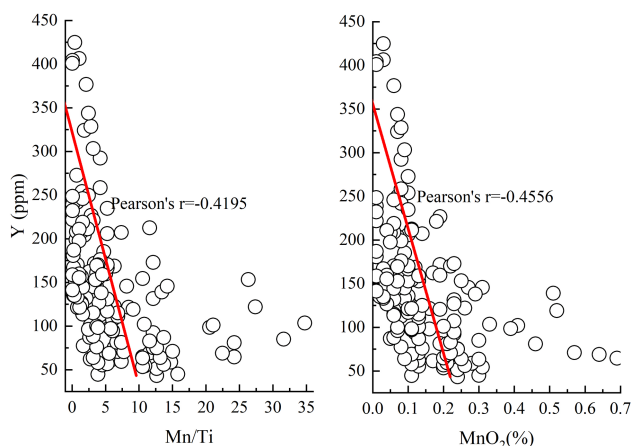


Fig. 16 Scatter plots of Y vs. Mn/Ti, Y vs. MnO₂ in Zhijin phosphorites

namely, LREEs enrichment and HREEs depletion. The properties of Y are special; however, because of the different removal effects in different environments of the solution, Y sometimes behaves similarly to HREEs and sometimes similar to LREEs (Borkowski and Siekierski 1992; Quinn et al. 2004). The properties of Y made it possible to approximate the nature of LREEs in the Early Cambrian Zhijin phosphorite, and Y shows even more covalent tendencies than LREEs. As a consequence, Y was highly enriched and deposited, and it became the richest rare element in this area. Consequently, the source for Y may have been from a series of original geological processes such as weathering, transport, placement, and so forth, but after sedimentary diagenesis, the enrichment of Y was rarely affected by post-diagenetic reworking.

In general, REYs in the Zhijin phosphorites showed an original signature, no Eu anomaly, no correlation between the hydrothermal elements and the ratios of hydrothermal elements with Y. Additionally, the paleogeography of Zhijin phosphorites was on the continental shelf, far from the Mid-Ocean Ridge, and thus, the seafloor hydrothermal activity did not directly provide the source of Y. Studies have revealed that the modern ocean floor is rich in rare earth especially Y (Takaya et al. 2018). Up-swelling currents transport rare earths and Y from the bottom of the ocean to the shallow sea (Hein et al. 2004), which results in the direct origin of some rare earth elements from seawater. Y in deep-sea mud exists principally in the form of phosphate and appears completely in apatite minerals, and the occurrence state of Y is similar to that in terrestrial phosphorites (Zhang et al. 2018). Through the investigations of Y/Ho ratios, Er/Nd ratios, and so on, it is proposed that the enrichment of Y exists because of the addition of a terrigenous source. Hence, the source for Y was the result of a mixture of seawater and terrestrial sources.

8 Conclusions

From the above discussion, the following conclusions were drawn:

- (1) According to the statistical analysis of the sample data, the Y in Zhijin rare earth-bearing phosphorite has normal distribution characteristics.
- (2) In Zhijin rare earth-bearing phosphorite, Y is especially enriched relative to other REYs elements. But in different $\sum \text{REY}$ intervals, the enrichment degree of Y is different relative to its neighbor elements. When the value of $\sum \text{REY}$ is smaller, the enrichment degree of Y is larger relative to its neighbor elements Dy and Ho; when the value of

$\sum \text{REY}$ is higher, the enrichment degree of Y is smaller relative to its neighbor elements Dy and Ho.

- (3) The analysis of the parameters of major and trace elements suggests that Zhijin rare earth-bearing phosphorite has the signature of primary phosphorite.
- (4) The results of the clustering and factor analysis show that, for the phosphorite with a low rare earth content (< 535 ppm), there is a good correlation between REEs, Y, and P_2O_5 . For the phosphorite with a high rare earth content (≥ 535 ppm), there is also a good correlation between REEs and P_2O_5 , but there is no correlation between Y and P_2O_5 . The REYs enrichment in the Zhijin rare earth-bearing phosphorite revealed that superposition enrichment may occur for Y. The inconsistent enrichment processes of REYs may be correlated with more complex sources of Y.
- (5) The data analysis of the Eu anomalies, representative elements of submarine hydrothermal activity and ratios of hydrothermal elements, REYs distribution patterns, and values of Y/Ho, Er/Nd, Mn/Ti, and MnO_2 show that submarine hydrothermal activity did not directly provide the source for Y, Y came from a mixture of seawater and terrestrial sources.

Acknowledgements We thank Prof. Jianzhong Liu for his helpful comments. This work is jointly supported by the National Natural Science Foundation of China (No. U1812402) and the Public Beneficial and Basic Geological Project from the Department of Land and Resources of Guizhou Province (No. 2016-09-1).

References

- Abedini A, Calagari AA (2017) REEs geochemical characteristics of lower Cambrian phosphatic rocks in the Gorgan-Rasht Zone, northern Iran: Implications for diagenetic effects and depositional conditions. *J Afr Earth Sci* 135:115–124
- Adachi M, Yamamoto K, Sugisaki R (1986) Hydrothermal chert and associated siliceous rocks from the northern Pacific their geological significance as indication of ocean ridge activity. *Sediment Geol* 47:125–148
- Bau M, Dulski P (1996) Distribution of yttrium and rare-earth elements in the Penge and Kuruman iron-formations, Transvaal Supergroup, South Africa. *Precambrian Res* 79:37–55
- Bau M, Möller P, Dulski P (1997) Yttrium and lanthanides in eastern Mediterranean seawater and their fractionation during redox-cycling. *Mar Chem* 56:123–131
- Bau M, Dulski P (1999) Comparing yttrium and rare earths in hydrothermal fluids from the Mid-Atlantic Ridge: implications for Y and REE behaviour during near-vent mixing and for the Y/Ho ratio of Proterozoic seawater. *Chem Geol* 155:77–90
- Borkowski M, Siekierski S (1992) Factors affecting the position of Y and actinides (III) with respect to lanthanides in the NH_4SCN -Adogen-564SCN extraction system. *Radiochim Acta* 56:31–35

- Chen JY, Yang RD, Wei HR, Gao JB (2013) Rare earth element geochemistry of Cambrian phosphorites from the Yangtze Region. *J Rare Earths* 31:101–112
- Chen JY (2019) Study on the occurrence state of rare earth element yttrium in Zhijin phosphate deposit-bearing rare earth based on synchrotron radiation XAFS experiment. *Proc 17th Ann Conf Chin Soc Mineral Petrol Geochem* 2:208–209 (in Chinese)
- Chew DM, Babechuk MG, Cogné N et al (2016) (LA, Q)-ICPMS trace-element analyses of Durango and McClure Mountain apatite and implications for making natural LA-ICPMS mineral standards. *Chem Geol* 435:35–48
- Douville E, Bienvenu P, Charlou JL, Donval JP, Fouquet Y, Appriou P, Gamo T (1999) Yttrium and rare earth elements in fluids from various deep-sea hydrothermal systems. *Geochimica et Cosmochimica Acta* 63:627–643
- Duan KB, Wang DH, He HJ, Zheng GD, Xiong XX, Yuan JG, He BB, Qu YY (2015) Study on geochemical characteristics of rare earth elements of xinhua phosphate rocks in the Upper Yangtze, South China by ICP-MS/AES and Its Sedimentology Implications. *Rock and Mineral Analysis* 34:261–267 (in Chinese with English abstract)
- Fazio AM, Scasso RA, Castro LN, Carey S (2007) Geochemistry of rare earth elements in early-diagenetic Miocene phosphatic concretions of Patagonia, Argentina: phosphogenetic implications. *Deep Sea Res. Part II* 54:1414–1432
- Ge DY, Liu YX, Zeng YF (1994) A discussion on weathering indexes of phosphorus ore from eastern Yunnan and the weathering process of phosphorite. *J Mineral Petrol* 14:29–42 (in Chinese with English abstract)
- George D, Mallery P (2019) IBM SPSS statistics 26 step by step: a simple guide and reference. Routledge, London
- Guo HY (2017) Geological Features and REE Ore-controlling Factors of Xinhua Phosphorite Type Rare-earth Deposit. Guiyang, Guizhou Province. Institute of Geochemistry, Chinese Academy of Sciences, Guizhou Province (in Chinese with English abstract)
- Guo HY, Xia Y, He S, Xie ZJ, Wei DT, Lei B (2017) Geochemical Characteristics of Zhijin Phosphorite Type Rare-earth Deposit, Guizhou Province, China. *Acta Mineral Sin* 37:755–763 (in Chinese with English abstract)
- Hein JR, Perkins RB, McIntyre BR (2004) Chapter 2 Evolution of thought concerning the origin of the phosphoria formation, western US phosphate field. *Handbook Explor Environ Geochem* 8:19–42
- Hein JR, Koschinsky A, Mikesell M, Mizell K, Glenn CR, Wood R (2016) Marine phosphorites as potential resources for heavy rare earth elements and Yttrium. *Minerals* 6:1–22
- Hekinian R, Fouquet Y (1985) Volcanism and metallogenesis of axial and off-axial structures on the East Pacific Rise near 13°N. *Econ Geol* 80:221–249
- Ilyin AV (1998) Rare-earth geochemistry of ‘old’ phosphorites and probability of syngenetic precipitation and accumulation of phosphate. *Chem Geol* 144:243–256
- Jiang XD, Sun XM, Chou YM, et al (2020) Geochemistry and origins of carbonate fluorapatite in seamount Fe-Mn crusts from the Pacific Ocean. *Marine Geology* 423
- Li LY, Li L, Zhao ZX, Li XK (2008) The basic trellis and its characters of the geologic structure in Zhijin. *Guizhou Geology* 25:35–40 (in Chinese with English abstract)
- Marchig V, Gundlach H, Möller P, Schley F (1982) Some geochemical indicators for discrimination between diagenetic and hydrothermal metalliferous sediments. *Mar Geol* 50:241–256
- Mao T, Yang RD, Gao JB, Mao JR (2015) Study of sedimentary feature of Cambrian phosphorite and ore-controlling feature of old karst surface of the Dengying formation in Zhijin. *Guizhou Acta Geol Sin* 89:2374–2388 (in Chinese with English abstract)
- McArthur JM, Coleman ML, Bremner JM (1980) Carbon and oxygen isotopic composition of structural carbonate in sedimentary francolite. *J Geol Soc London* 137:669–673
- McArthur JM, Walsh JN (1984) Rare-earth geochemistry of phosphorites. *Chem Geol* 47:191–220
- McArthur JM, Benmore RA, Coleman ML, Soldi C, Yeh HW, O’Brien GW (1986) Stable isotopic characterisation of francolite formation. *Earth Planet. Sci Lett* 77:20–34
- McLennan SM (1989) Rare earth elements in sedimentary rocks: influence of provenance and sedimentary processes. *Rev Mineral Geochem* 21:169–200
- Meng QT, et al. (2016) Complete exploration report of phosphorite (rare earth) ore in Zhijin area, Guizhou province. Guizhou Guiyang: 104 Geological Brigade of Bureau of Geology and Mineral Exploration and Development of Guizhou Province (in Chinese)
- Morad S, Felitsyn S (2001) Identification of primary Ce-anomaly signatures in fossil biogenic apatite: implication for the Cambrian oceanic anoxia and phosphogenesis. *Sediment Geol* 143:259–264
- Nozaki Y, Zhang J, Amakawa H (1997) The fractionation between Y and Ho in the marine environment. *Earth Planet. Sci Lett* 148:329–340
- Emsbo P, McLaughlin PI, Breit GN, du Bray EA, Koenig AE (2015) Rare earth elements in sedimentary phosphate deposits: solution to the global REE crisis? *Gondwana Res* 27:776–785
- Quinn KA, Byrne RH, Schijf J (2004) Comparative scavenging of yttrium and the rare earth elements in seawater: competitive influences of solution and surface chemistry. *Aquat Geochem* 10:59–80
- Shields G, Stille P (2001) Diagenetic constraints on the use of cerium anomalies as palaeoseawater redox proxies: an isotopic and REE study of Cambrian phosphorites. *Chem Geol* 175:29–48
- Siekierski S (1981) The position of yttrium within lanthanides with respect to unit cell volumes of isostructural compounds as an indication of covalency in lanthanide compounds. *J Solid State Chem* 37(3):279–283
- Stine RA (2016) Explaining Normal Quantile-Quantile Plots Through Animation: The Water-Filling Analogy. *Am Stat* 71:145–147
- Takaya Y, Yasukawa K, Kawasaki T et al (2018) The tremendous potential of deep-sea mud as a source of rare-earth elements. *Sci Rep* 8:3406–3414
- Tan QP, Wang XQ (2017) Temporal-spatial distributions of gold in drainage sediments and rocks in the Qinling region, China. *Bull Mineral Petrol Geochem* 36:132–141 (in Chinese with English abstract)
- Tan QP, Wang XQ et al. (2018) Identifying ore-related anomalies using singularity mapping of stream sediment geochemical data, a case study of Pb mineralization in the Qinling region, China. *Geochem Explor Environ A* 18:177–184
- Taylor SR, McLennan SM (1985) The continental crust: its composition and evolution. Blackwell, Oxford, p. 321
- Tian JC, Zhang X (2016) Sedimentary geochemistry. Geological Publishing House, Beijing, pp 46–47 (in Chinese)
- Wu SW (2019) Study on REE enrichment characteristics and economic index of mineral exploration in phosphorite-type REE deposit in Zhijin, Guizhou province. Dissertation, Institute of Geochemistry, Chinese Academy of Sciences (in Chinese with English abstract)
- Wu SW, Xia Y, Tan QP, Xu JB, Xie ZJ, Yang HY, He S (2019) The REE geochemical characteristics and REE enrichment of ore-bearing rocks of the Zhijin phosphorite-type REE deposit, Guizhou, China. *Acta Mineral Sin* 39:359–370 (in Chinese with English abstract)

- Xia Y, Xie ZJ, Zhang H, Xiao JF (2019) A report on the results of research on ore-forming rules and economic indexes of ore exploration technology and deposit exploration in Zhijin phosphorite-type rare earth ore in Guizhou Province. Institute of Geochemistry, Chinese Academy of Sciences, Guiyang, Guizhou Province **(in Chinese)**
- Xu JB (2019) The Research of the Law and Paleogeographic Environmental Constraints of Rare Earth Element Enrichment of Phosphorite-type Rare Earth Ore in Zhijin, Guizhou Province. Dissertation, Institute of Geochemistry, Chinese Academy of Sciences (in Chinese with English abstract)
- Xu JB, Xiao JF, Yang HY, Xia Y, Wu SW, Xie ZJ (2019) The REE enrichment characteristics and constraints of the phosphorite in Zhijin, Guizhou: a case study of No. 2204 drilling cores in the Motianchong ore block. *Acta Mineral Sin* 39:371–379 **(in Chinese with English abstract)**
- Yang WD, Qi L, Lu XY (1995) Geochemical characteristics and genesis of rare earth elements in the early Cambrian of eastern Yunnan. *Acta Mineral Sin* 4:224–227 **(in Chinese)**
- Yang J, He TY (2013) Zhijin county Guizhou province Xinhua containing-rare earth phosphorite rock deposit geological characteristics and reasons discussed. *Geol Chem Miner* 35:27–33 **(in Chinese with English abstract)**
- Yang HY (2020) A comparative study on metallogenic paleo-environments of phosphorites of the Doushantu and Gezhongwu formations in the Central Guizhou and their constraints on the enrichment of rare earth elements. Dissertation, Institute of Geochemistry, Chinese Academy of Sciences (in Chinese with English abstract)
- Ye LJ (1963) Study on ore-forming and extracting of exogenic deposits from continental sources. *Sci Geol Sin* 2:67–87 (in Chinese)
- Yi HS, Peng J, Xia WJ (1995) The late precambrian paleo-ocean evolution of the southeast Yangtze continental margin: REE record. *Acta Sedimentol Sin* 13:131–137 **(in Chinese with English abstract)**
- Zhang J, Chen DL (2000) Scanning electron microscope study of the ore-bearing REE in Xinhua phosphorite, Zhijin, Guizhou. *J Mineral Petrol* 20:59–64 **(in Chinese with English abstract)**
- Zhang J, Chen JY, Chen DL (2004) Characteristics of main material composition of phosphorite in Guizhou Province. *China Non-Metallic Miner Ind* 43:91–92 **(in Chinese)**
- Zhang J, Sun CM, Gong ML, Zhang Q, Chen DL, Chen JY (2007a) Geochemical characteristics and occurrence states of the REE elements of the phosphorite in Xinhua, Zhijin. *Guizhou J Rare Earths* 28:75–79 **(in Chinese with English abstract)**
- Zhang YB, Gong ML, Li H (2007b) Occurrence of REE in rare earth phosphorite in Zhijin area, Guizhou. *J Earth Sci Environ* 29:362–368 **(in Chinese with English abstract)**
- Zhang XL, Cui LH (2016) Oxygen requirements for the Cambrian explosion. *J Earth Sci* 27:187–195
- Zhang KF, Liu ZQ, Sun CY, Cao HY, Zhu KC, Zhu W, Li W (2018) Recovery of yttrium from deep-sea mud. *J. Rare Earths* 36:863–872